2013

Assessment and Recommendations for Using High-Resolution Weather Information to Improve Winter Maintenance Operations

Michael Baldwin
Purdue University, baldwin@purdue.edu

Kimberly Hoogewind
Purdue University, khoogewi@purdue.edu

Derrick Snyder
Purdue University, dwsnyder@purdue.edu

Matthew Price
Purdue University, pricemr@purdue.edu

R. Jeffrey Trapp
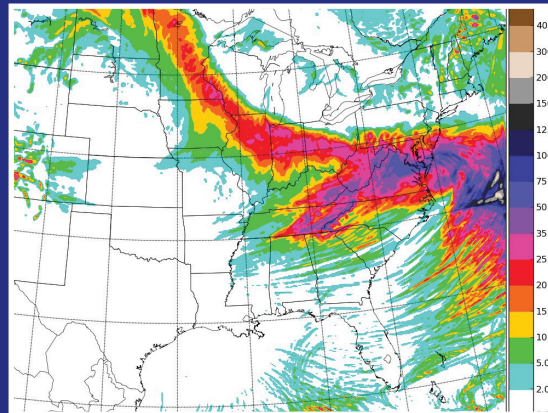*Purdue University*, jtrapp@purdue.edu

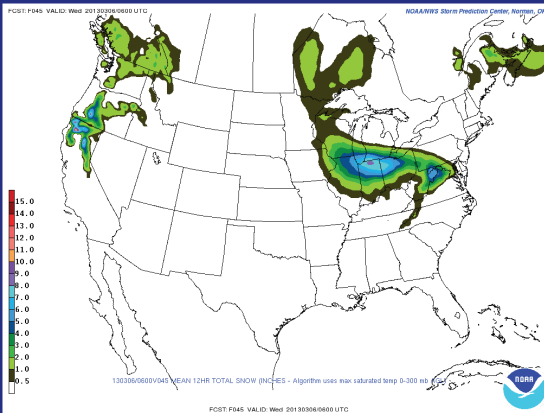# Assessment and Recommendations for Using High-Resolution Weather Information to Improve Winter Maintenance Operations

Michael Baldwin

Derrick Snyder

Kimberly Hoogewind

Matthew Price

R. Jeffrey Trapp

1. Report No.	2. Government Accession No.	3. Recipient's Catalog No.
FHWA/IN/JTRP-2013/22		

4. Title and Subtitle	5. Report Date
Assessment and Recommendations for Using High-Resolution Weather Information to Improve Winter Maintenance Operations	November 2013
	6. Performing Organization Code

7. Author(s)	8. Performing Organization Report No.
Michael Baldwin, Kimberly Hoogewind, Derrick Snyder, Matthew Price, R. Jeffrey Trapp	FHWA/IN/JTRP-2013/22

9. Performing Organization Name and Address	10. Work Unit No.
Joint Transportation Research Program Purdue University 550 Stadium Mall Drive West Lafayette, IN 47907-2051	
	11. Contract or Grant No. SPR-3718

12. Sponsoring Agency Name and Address	13. Type of Report and Period Covered
Indiana Department of Transportation State Office Building 100 North Senate Avenue Indianapolis, IN 46204	Final Report
	14. Sponsoring Agency Code

15. Supplementary Notes
Prepared in cooperation with the Indiana Department of Transportation and Federal Highway Administration.

16. Abstract

A variety of methods for obtaining detailed analyses regarding the timing and duration of winter weather across the state of Indiana for multiple seasons were compared and evaluated during this project. Meteorological information from sources such as surface reporting stations, National Weather Service radars, and three-dimensional weather analysis and prediction systems were utilized in this work. In addition, daily weather forecasts were provided by students at Purdue University during the 2012-13 winter season. These forecasts supplemented the weather forecast information already in use at INDOT. Purdue weather forecasts were systematically evaluated during this project. The results from these assessments are provided in this report, along with a set of recommendations for sources of detailed weather information to be utilized by INDOT in future winter seasons.

17. Key Words	18. Distribution Statement
winter maintenance, road weather analysis, road weather forecasting	No restrictions. This document is available to the public through the National Technical Information Service, Springfield, VA 22161.

19. Security Classif. (of this report)	20. Security Classif. (of this page)	21. No. of Pages	22. Price
Unclassified	Unclassified	42	

Form DOT F 1700.7 (8-69)

AUTHORS

Michael Baldwin, PhD
Associate Professor
Department of Earth, Atmospheric, and Planetary Sciences
Purdue University
(765) 494-0345
baldwin@purdue.edu
Corresponding Author

Kimberly Hoogewind
Graduate Research Assistant
Department of Earth, Atmospheric, and Planetary Sciences
Purdue University

Derrick Snyder
Graduate Research Assistant
Department of Earth, Atmospheric, and Planetary Sciences
Purdue University

Matthew Price
Undergraduate Research Assistant
Department of Earth, Atmospheric, and Planetary Sciences
Purdue University

R. Jeffrey Trapp, PhD
Associate Professor
Department of Earth, Atmospheric, and Planetary Sciences
Purdue University

JOINT TRANSPORTATION RESEARCH PROGRAM

The Joint Transportation Research Program serves as a vehicle for INDOT collaboration with higher education institutions and industry in Indiana to facilitate innovation that results in continuous improvement in the planning, design, construction, operation, management and economic efficiency of the Indiana transportation infrastructure. https://engineering.purdue.edu/JTRP/index_html

Published reports of the Joint Transportation Research Program are available at: http://docs.lib.purdue.edu/jtrp/

NOTICE

The contents of this report reflect the views of the authors, who are responsible for the facts and the accuracy of the data presented herein. The contents do not necessarily reflect the official views and policies of the Indiana Department of Transportation or the Federal Highway Administration. The report does not constitute a standard, specification or regulation.

EXECUTIVE SUMMARY

ASSESSMENT AND RECOMMENDATIONS FOR USING HIGH-RESOLUTION WEATHER INFORMATION TO IMPROVE WINTER MAINTENANCE OPERATIONS

Introduction

Winter weather hazards (snow, freezing rain, bridge deck icing, etc.) often degrade road conditions and can result in substantial increases in travel time and accident frequency without proper treatment. The resources required for the Indiana Department of Transportation's (INDOT's) winter maintenance operations are currently estimated for the 2012–2013 season at over $30M. A large number of decisions related to treatment must be made given available information regarding the previous, current, and future weather conditions that often contain considerable uncertainty. It is expected that more accurate and precise weather information will help to reduce the uncertainty related to winter weather, resulting in improved decision-making and significant cost savings for winter operations.

In this project, state-of-the-art weather information from radar and meteorological data analysis systems were evaluated to determine which would provide accurate high-resolution ($\sim$5 km scale) information to assist with after-action review of previous seasons as well as the analysis of current weather situations. In addition, detailed weather forecasts were provided to INDOT by Purdue students, utilizing a high-resolution numerical weather prediction model. These forecasts were in the form of probabilistic maps and timelines of winter weather hazards for each INDOT district, along with a written discussion for each forecast. The outcome of this research is a set of recommendations regarding implementation of more detailed weather information related to winter weather decision-making at INDOT. By working directly with INDOT "customers," a large number of Purdue meteorology students have gained a rich learning experience by executing a complete "forecast process."

Findings

Several state-of-the-art weather analyses were evaluated and compared against surface weather station observations to determine which system would generate weather hour estimates that were both accurate and spatially detailed. The RTMA-based analyses underestimated weather hours and also contained analysis artifacts (circular patterns) that were unrealistic. The NMQ-based analyses over-estimated weather hours, especially within $\sim$75 miles of a radar site, except for a narrow circle centered at each NWS radar location. The NWS dual-pol radar products were found to be immature with the precipitation type classification algorithm containing several major errors. The RAP-based weather hour analyses matched up well against the surface station data and also provided more realistic spatial detail. These analyses are recommended for use for after-action review both for previous and upcoming winter seasons.

Daily winter weather forecasts were provided to INDOT by Purdue students (under the supervision of Professor Baldwin). These forecast products were evaluated and found to be skillful and unbiased in predicting the occurrence of snow in particular. Purdue students (and professors) gained a rich learning experience as a result of their interaction with their INDOT "customers." It is recommended that Purdue continues to communicate this kind of weather forecast information to INDOT for upcoming winter seasons.

High-resolution numerical weather prediction model output was also incorporated into these experimental forecast products. These numerical forecasts were found to be very useful by the Purdue student forecasters. It is recommended that Purdue continues to evaluate and develop numerical weather forecasts for road weather purposes, working with INDOT's weather vendor to provide direct access to this alternate source of forecast information, resulting in increased confidence and improved decision-making for winter maintenance.

Implementation

New spatially detailed datasets for analyzing winter weather hours across the state will be provided to INDOT in a form that will allow easy implementation into INDOT operations. We recommend that INDOT begin using the more detailed analysis datasets to analyze the performance of maintenance operations for upcoming and previous winter seasons. Numerical forecast information from the high-resolution weather prediction model run at Purdue should also be made accessible to INDOT via MDSS. Student-generated weather forecasts designed for direct use in INDOT winter maintenance decision-making will continue, taking into account the forecast information available from multiple sources.

One of the main results from the evaluation of Purdue's experimental weather forecasts was that these forecasts were, on average, unbiased in terms of the frequency of occurrence of snow at the district level. Unbiased forecasts, or forecasts that neither over-forecast nor under-forecast the frequency of winter weather conditions, should help to minimize unnecessary costs due to extra man hours/overtime. In addition, it should improve analysis of costs per lane mile per weather hour, allowing the potential for more uniform (and cost-effective) operations statewide.

CONTENTS

LIST OF TABLES

1. INTRODUCTION

Winter weather hazards (for example: snow, freezing rain, bridge deck icing) often degrade road conditions and can result in substantial increases in travel time and accident frequency (*1*) without proper treatment. The resources required for INDOT's winter maintenance operations are currently estimated for the 2012–2013 season at over $30M. A large number of decisions related to treatment must be made given available information regarding the previous, current, and future weather conditions that often contain considerable uncertainty. It is expected that more accurate and precise weather information will help to reduce the uncertainty related to winter weather, resulting in improved decision-making and significant cost savings for winter operations. State-of-the-art weather information from radar and meteorological data analysis systems can provide high-resolution (~5 km scale) information and help with after-action review of previous seasons as well as the analysis of current weather situations, producing improvements in the winter treatment decision-making process as a result.

The weather forecasting process can be described as a system where information flows from one task to another, reducing uncertainty about the current and future weather conditions. These tasks can be generally denoted as *monitoring*, *forecasting*, *communication*, and *evaluation*. The task of *monitoring* weather conditions involves collecting observations related to the current and previous weather events and analyzing those observations in order to generate a coherent picture of the variables that best describe what is happening in the weather as well as explaining why it is happening. The *forecasting* task involves taking that coherent picture of the current weather conditions and using knowledge of how the atmosphere changes with time to predict future weather conditions. This task usually involves a variety of complex numerical models that contain both systematic and random errors; therefore an ensemble of possible future outcomes is typically produced. A good forecaster will consider both the most likely outcome as well as the range of potential outcomes in generating their forecast. Once the forecaster has performed this analysis of the information, they can communicate this information to their end users and describe what will happen as well as explain why it is going to happen. This is the *communication* task; a good forecaster will effectively communicate their understanding to their customers, the users of the forecast information. The *evaluation* task involves analyzing what actually happened once the forecast is complete, as well as understanding why it happened. Predictions will always contain errors and this "after-action review" is the most effective way that a forecaster can improve upon their forecasting process. The information obtained during the evaluation task will feed back into the forecasting process to improve future predictions.

1.1 Problem Statement

Weather conditions vary considerably in time and space across the state of Indiana. During the winter, it is not unusual to find drastically different conditions over a distance as small as a single Indiana county. The weather information currently used by INDOT to estimate the number of winter weather hours that impact each segment of the state is lacking in spatial detail. These spatially-smooth weather hour estimates make it very difficult to accurately assess the costs of winter maintenance per lane mile, per weather hour. In addition, INDOT staff utilizes a wide variety of sources of weather forecasting information, but receive very little (if any) information regarding the physical reasoning and degree of uncertainty associated with those forecasts, thereby increasing the difficulty in critical decision-making for winter road maintenance. These problems can be ameliorated via implementation of more detailed and informative weather data products that are designed to assist with winter weather decision-making at INDOT.

1.2 Objectives

Our research objective in this work was to provide more detailed and specific forms of weather information intended for monitoring and predicting winter weather conditions, and to assess the quality of the more detailed weather information. The outcome of this research is a set of recommendations regarding implementation of more detailed weather information related to winter weather decision-making at INDOT. By working directly with INDOT "customers," a large number of Purdue meteorology students have gained a rich learning experience by executing a complete "forecast process."

1.3 Work Plan

In order to accomplish these objectives, during this project we:

1. Developed alternative winter weather hour analysis data sets using high-resolution (in both space and time) radar data and analyses of meteorological observations. These alternative data sets were developed in three stages:

   - Stage I: utilizing surface-based weather observing sites
   - Stage II: utilizing high-resolution gridded analyses of weather variables
   - Stage III: utilizing dual-polarimetric Doppler radar data

2. Provided experimental winter weather forecast information by developing a high-resolution weather prediction system.
3. Evaluated the experimental weather hour analyses and forecast information, resulting in a set of recommendations for implementation into INDOT winter maintenance operations.

The results of this work will be presented in the upcoming "Analysis of Data" sections of this report.

Section 1 of the data analysis will present the Stage I–III winter weather hour analyses. Section 2 will discuss the experimental weather forecast information as well as the evaluation of these products. The data analysis will be followed by concluding sections, including recommendations for implementation, and identification of the project deliverables.

2. ANALYSIS OF DATA: SECTION 1—WINTER WEATHER HOURS

2.1 "Stage I" Observation-Based Analyses of Winter Weather for the 2010–2013 Seasons

2.1.1 Data Sources

2.1.1.1 2010–2012 Seasons. Analyses of winter weather hours for the 2010–2012 seasons were calculated using surface weather stations. These surface observations were interpolated onto a grid using ArcGIS software. Four criteria were used to identify suitable weather station data to calculate winter weather hours:

1. Hourly weather data with variables that can be used to calculate or infer winter weather hazards (temperature, precipitation, freezing fog, and blowing snow);
2. Spatial distribution of weather stations;
3. Temporal resolution (i.e., no missing data);
4. Data quality.

Using these criteria, three potential sources of hourly weather observations were identified:

1. National Climatic Data Center (NCDC): Quality controlled, hourly airport weather data collected by Automated Surface Observing System (ASOS);
2. Meteorological Assimilation Data Ingest System (MADIS): Supplemental weather data from lower complexity but more numerous weather stations allowing for better spatial distribution;
3. Indiana State Climate Office (IClimate): Hourly weather observations from Purdue's agricultural research stations around the state.

NCDC data contain temperature, precipitation, precipitation type, and visibility variables on an hourly basis. MADIS and IClimate data only contain hourly temperature and hourly precipitation variables. NCDC data were used to calculate non-precipitating winter weather hours (freezing fog and blowing snow). To encompass all possible winter weather hours, a temperature threshold was used: If a station reported any measurable precipitation (0.01" or greater) and a temperature at or below the temperature threshold during an hour, that hour was counted as a *winter weather hour*. A temperature threshold of 32°F was selected. Interpolations of precipitating and non-precipitating winter weather hours for a season were done separately then combined. Table 2.1 summarizes the number of point data by data source for each season.

TABLE 2.1
Number of Stations per winter season

Season	NCDC	MADIS	IClimate	Total
2009–2010	31	0	7	38
2010–2011	31	0	6	37
2011–2012	48	8	7	63

2.1.1.2 2013 Season. For the 2012–2013 season, a frequency analysis of various types of wintry precipitation was conducted using ASOS data from NCDC and the Indiana State Climate Office. As with the other seasons, data availability and continuity were the main criteria in station selection. These point values were interpolated onto a 20 km × 20 km grid using the IDW function in ArcMap, as described previously. Table 2.2 shows the variables that were interpolated, and Figure 2.1 shows the locations of the ASOS. The different types of precipitation that were analyzed follow the observed reports of present weather conditions provided by the National Weather Service. The National Weather Service uses visibility thresholds to define different categories of snow intensity. Light snow is reported when the visibility is greater than ½ mile, moderate snow is reported with visibilities less than or equal to ½ mile and greater than ¼ mile, and heavy snow is reported when the visibility is less than or equal to ¼ mile.

2.1.2 Methods

To ensure that data interpolation was performed over the same area, a study area was defined around Indiana. In the environmental variables of each interpolation model, the study area was set as the processing extent. Over Lake Michigan, there is a large gap in coverage where no useable weather data exists. To prevent this gap from interfering with the interpolation of areas near Lake Michigan, an interpolation barrier was placed along the southern shore of the lake. The study area and interpolation barrier are outline in Figure 2.2.

To interpolate the point observations into gridded data for each season, inverse distance weighting (IDW) interpolation was used. This interpolation method uses smoothing parameter and a search radius. Inverse distance weighted interpolation is a linear interpolation function that calculates a value at a grid point based on an average of surrounding point values weighted by the inverse of the distance from the point observation to the grid point. A smoothing function, selected by the user, controls the significance of point values farther away from a grid point. The mathematical basis for the IDW function in ArcMap is given by $Z_p = \dfrac{\sum \left(\dfrac{Z}{d_n}\right)}{\sum \left(\dfrac{1}{d_n}\right)}$ where Z_p is the analysis value at a grid point, Z is a point observation, d is the distance from a point observation

TABLE 2.2
ASOS observations used in 2013 season interpolations

Precipitation Type	Snow	Snow	Snow	Ice Pellets	Freezing Rain	Freezing fog	Blowing snow	Rain
Intensity	Light	Moderate	Heavy	Any	Any	Any	Any	Any

to Z_p and n is a power function of d which acts as a smoothing parameter (2). The user has control over the number of point observations that are used in the interpolation of a grid point value. A user can designate a fixed number of points to be interpolated, or the user can define a radius of influence in which only the points that fall within the radius are used in interpolation.

For the 2010–2012 season analyses, the default smoothing parameter (2.0) was used. A variable search radius of the 12 nearest observations to a grid point was used in interpolation. For the 2013 season analysis, cross-validation was used to determine an optimal smoothing parameter. The cross-validation tool in

ArcMap removes one data point at a time in the analysis space, performs the IDW interpolation without the data value and compares the interpolated value at the location of the missing point value to the actual point value. This process is continued for all data points and for all possible smoothing parameter values (3). Error in the predicted interpolation is quantified by calculating root mean square error and is known as
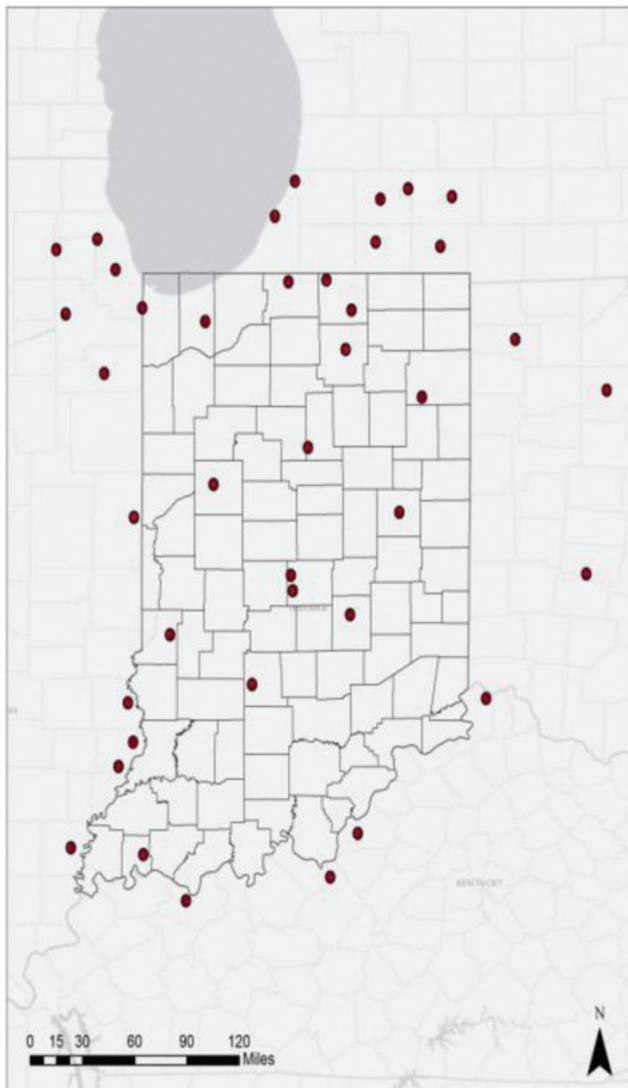
Figure 2.1 Locations of ASOS used in interpolation.

Study Area and Barrier
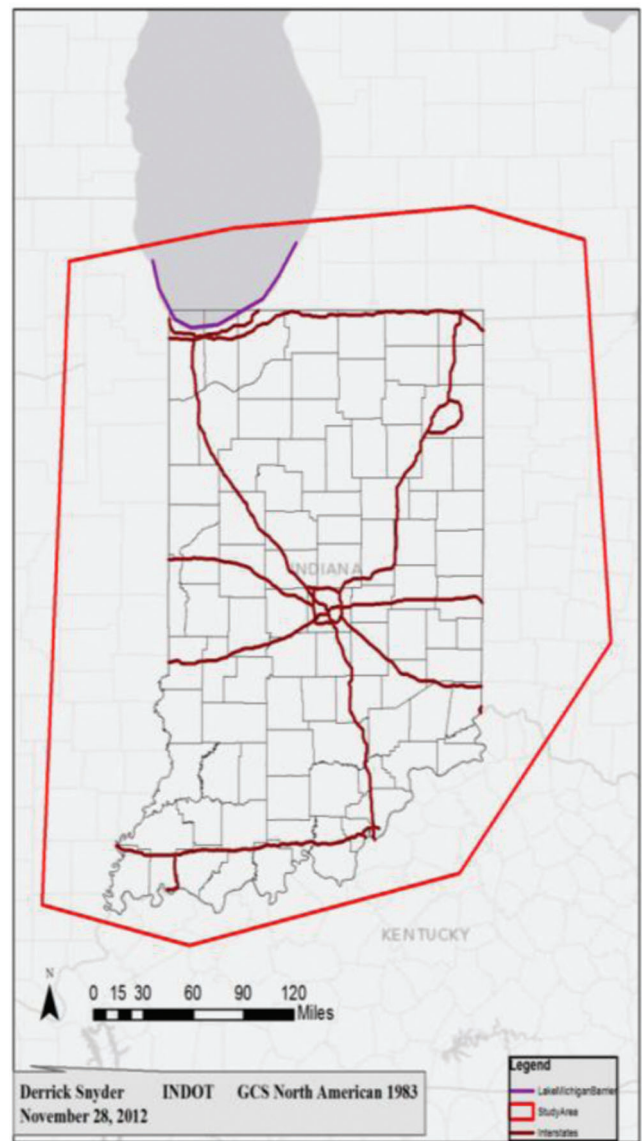
Figure 2.2 Study area and interpolation barrier. The study area was also set as the processing extent for the interpolations.

TABLE 2.3
Ideal smoothing parameters calculated using cross-validation

Precipitation Type	Light snow	Moderate snow	Heavy snow	Ice pellets	Freezing rain	Freezing fog	Blowing snow	Rain
Smoothing Parameter	2.0	3.1	1.3	1.0	1.1	1.0	1.0	1.0

root mean square prediction error (4). The cross-validation method for interpolated ASOS observations showed ideal smoothing parameter values between 1.0 and 3.1 (Table 2.3).

Since the number of ASOS stations is relatively few (40) and considering the localized influence that Lake Michigan can have on winter precipitation in northern Indiana via lake-effect precipitation, a fixed search radius was used to determine the number of point values used in the interpolation of a grid point. To determine an ideal search radius, an analysis of station spacing was performed. The largest minimum distance from one station to another was found to be ~100 km. Therefore a 100 km search radius was used. This ensured that there would be no areas of missing data in the interpolation and that point data near Lake Michigan would be used in interpolating grid points in areas that are not influenced by the lake.

2.1.3 Results and Discussion

2.1.3.1 Stage I Analyses of the 2010–2012 Seasons. Stage I winter weather hour analyses for the 2010 to 2012 seasons are shown in Figures 2.3, 2.4, and 2.5. Comparing data from the four winter seasons, variability was seen in the absolute magnitude of winter weathers by each season. However, general patterns were noted in the interpolations: Lowest values of winter weather hours were found along the Ohio
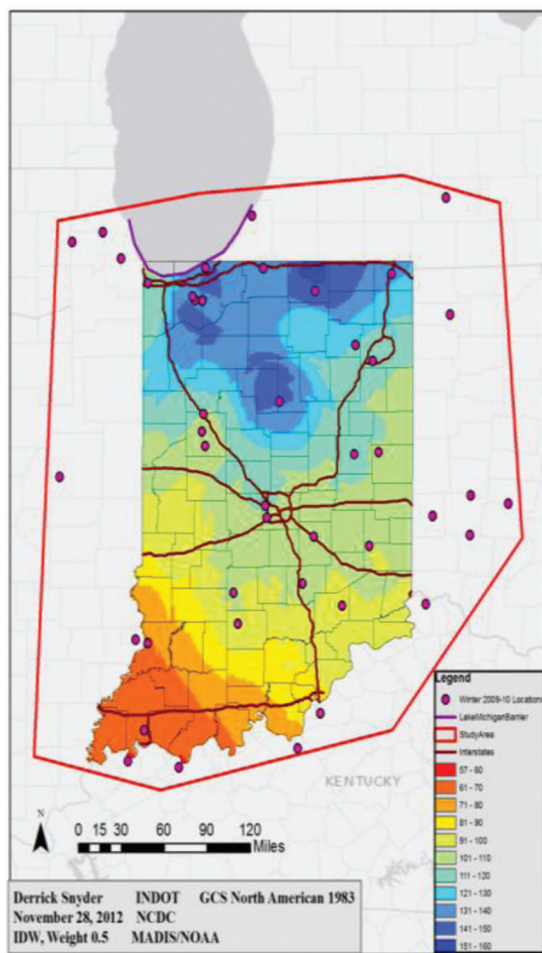
Figure 2.3 "Stage I" observation-based analysis for the 2010 winter season.
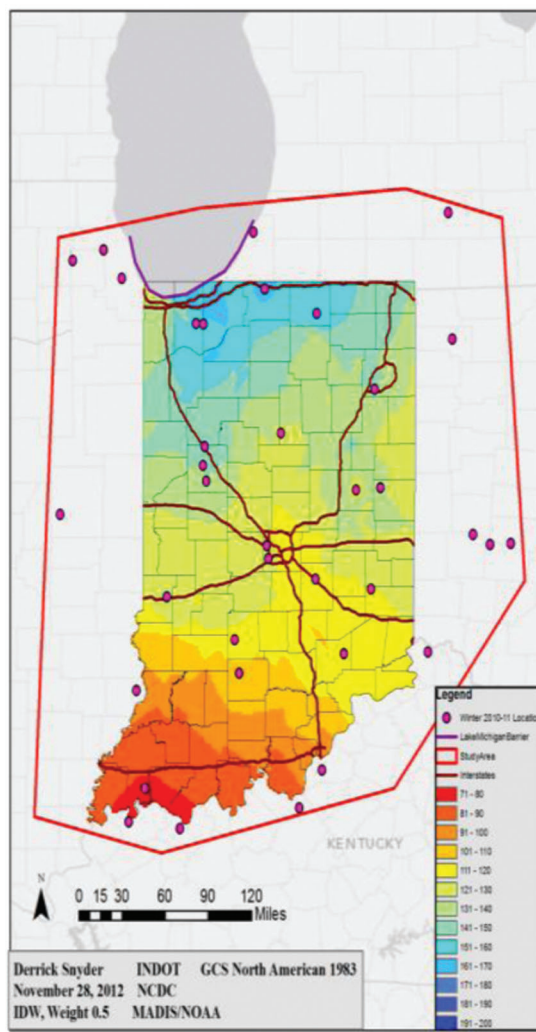
Figure 2.4 "Stage I" observation-based analysis of the 2011 season.

River in southern Indiana, increasing to a maximum near South Bend and near Lake Michigan in northern Indiana. The average value of precipitating winter weather hours was found to be about ten times greater than non-precipitating winter weather hours in general, making precipitating winter weather hours the dominant feature in the interpolation analysis. The 2011 season analysis saw the most winter weather hours statewide, while the 2012 season analysis showed the fewest numbers of winter weather hours. Stage I analyses were created in a similar fashion to winter weather hour estimates made for INDOT for previous seasons, except with a larger number of surface weather stations. Overall, incorporating extra stations into winter weather hour calculation did not dramatically alter the analyses when INDOT's winter weather hour estimates were informally compared with the Stage I analyses. However, some enhancement and refinement in the analyses were seen, especially in areas prone to lake effect snow in northern Indiana. This enhanced information can be useful in planning and evaluation purposes for winter operations.

2.1.3.2 Stage I Analyses of the 2013 Season. Plots of all interpolated results can be found in Figures 2.6 through 2.13 in order of their description in this section. Plots of interpolated hours of light snowfall (snow observed with visibility greater than ½ mile) showed increasing hours of snow from south (~100 hours) to north (~300 hours), with the highest hours of snowfall near and downwind of Lake Michigan, stretching east to the intersection of the Indiana, Michigan and Ohio borders. Hours of moderate snow (visibility greater than ¼ mile and less than or equal to ½ mile) showed less widespread lake effect influence, with a local
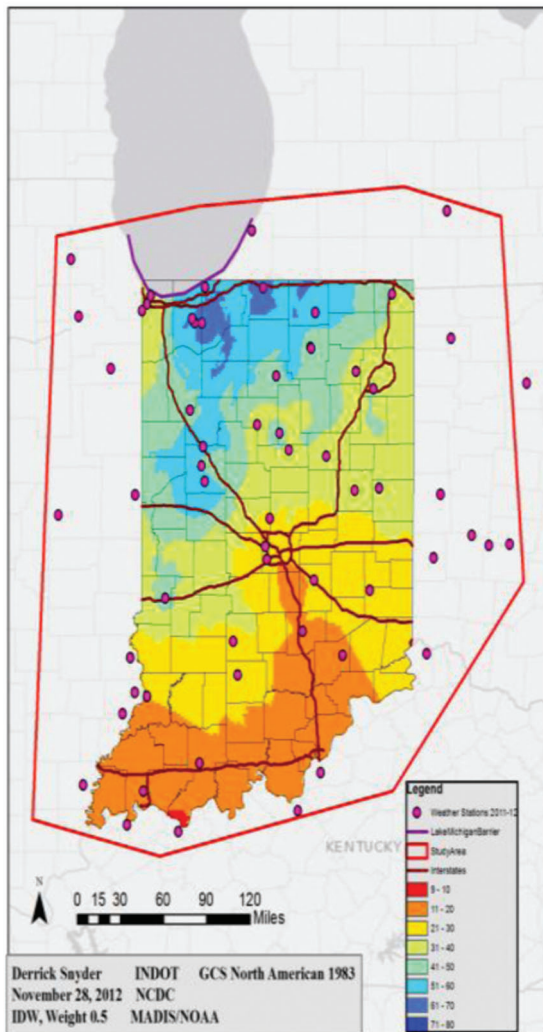
Figure 2.5 "Stage I" observation-based analysis of the 2012 season.

Figure 2.6 "Stage I" observation-based analysis of hours of light snow for the 2013 season.

Figure 2.7 "Stage I" observation-based analysis of hours of moderate snow for the 2013 season.

Figure 2.8 "Stage I" observation-based analysis of hours of heavy snow for the 2013 season.

maximum in hours (20–25 hours) of moderate snow around South Bend, Indiana. Other local maxima (16–20 hours) were noted near Muncie, Indiana, and Evansville, Indiana. Total hours of heavy snow reports (visibility less than or equal to ¼ mile) were few in general (total range of 0 to 6 hours); however, the most hours of heavy snow were found in east central Indiana, and did not exhibit an increase near Lake Michigan. This would imply that "heavy" lake effect snowfall did not occur during the winter; however a more plausible explanation is that the ASOS network spacing (avg. ASOS spacing is ~40 km) was too large to observe these snow bands. The most hours of rain were found in southern Indiana (250–300 hours) and decreased with increasing latitude (widespread < 100 hours in northern Indiana). No lake effect enhancement of rain was noted. Freezing rain was observed across the state, with the highest hours of observed freezing rain (11–15) were observed in pockets

in northwest and south central Indiana, with the fewest in northern and southwest Indiana. The most hours of freezing fog were observed in far southwest Indiana. This freezing fog was due to the melting of an extensive snowpack deposited by a snowstorm that occurred on 26 December 2012 in that region. Interpolation results for hours of ice pellets and hours of blowing snow are presented with much uncertainty and skepticism. Analyzing ASOS observations showed reports of very few reports of "ice pellets" but several reports of "precipitation falling, solid." Including this "unknown solid precipitation" variable allowed plots of ice pellets to be interpolated; however these values are most likely unusable. A similar case exists with hours of blowing snow. Only KCVG (Covington, Kentucky) reported any hours of blowing snow during the entire winter, which obviously created unrealistic interpolation results.

Despite the large grid spacing, much valuable information can be discerned from the figures, especially

Figure 2.9 "Stage I" observation-based analysis of hours of freezing fog for the 2013 season.

Figure 2.10 "Stage I" observation-based analysis of hours of freezing rain for the 2013 season.

when comparing the distributions of light to moderate to heavy snow. More analyses should be done to compare this season to other seasons using ASOS. Future work should include utilizing ASOS data to create a climatology of winter weather phenomena. This is complicated by a lack of continuous hourly observations for many ASOS stations.

2.2 "Stage II" Estimates of Winter Weather Hours for 2010–2013 Seasons

2.2.1 Data Sources and Methods

As a part of the monitoring portion of this project, winter weather hours were also estimated using high-resolution gridded analyses of weather variables for the past three winter seasons (2010–2013). Three separate datasets were used to compile these analyses:

1. Rapid Refresh (RAP)/Rapid Update Cycle (RUC) forecast systems
2. Real-Time Mesoscale Analysis (RTMA)
3. National Mosaic and Multi-Sensor QPE (NMQ) System

In order to maintain comparability between seasons, a winter season has been arbitrarily defined as the time period between November 1 and April 1. In addition to seasonal weather hour estimates, monthly and daily accumulations were also computed. A day was defined as the 24 hour period between 06–06 UTC (midnight–midnight CST) on two consecutive days. A more detailed description of the data and methods follow in the subsequent sections, while an intercomparison of results will be discussed in a later section. All data with the exception of NMQ were obtained from the National Climatic Data Center (NCDC), while NMQ was obtained from the National Severe Storms Laboratory (NSSL).
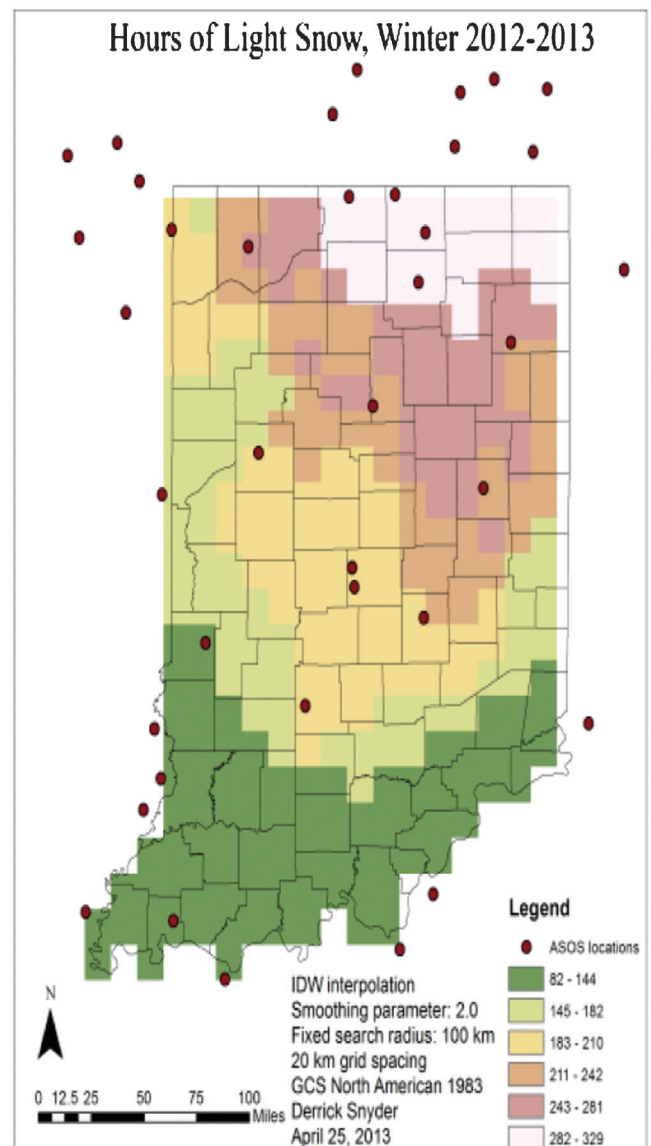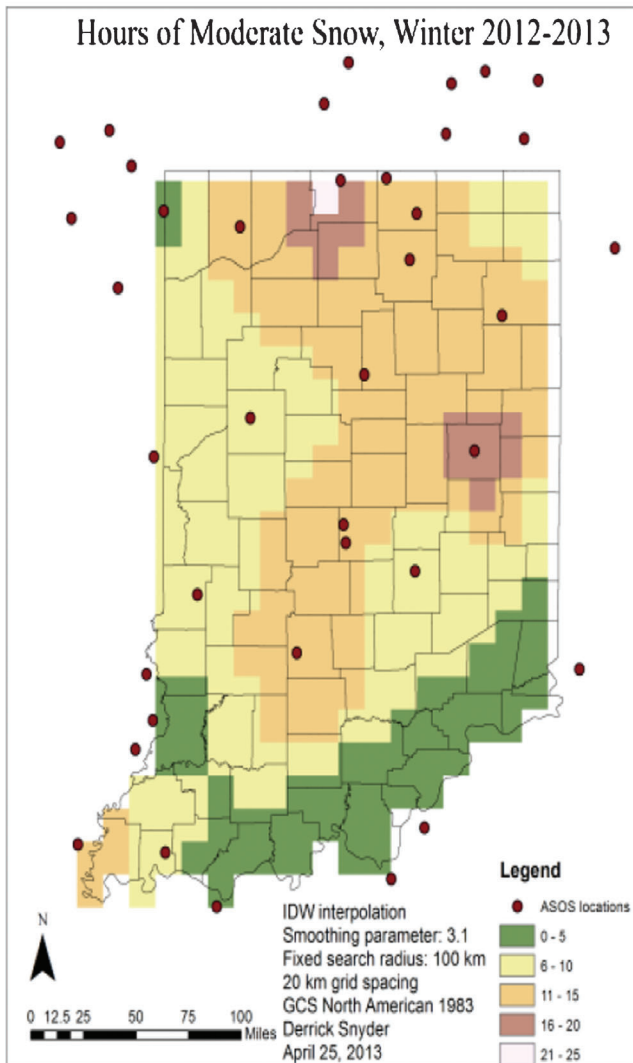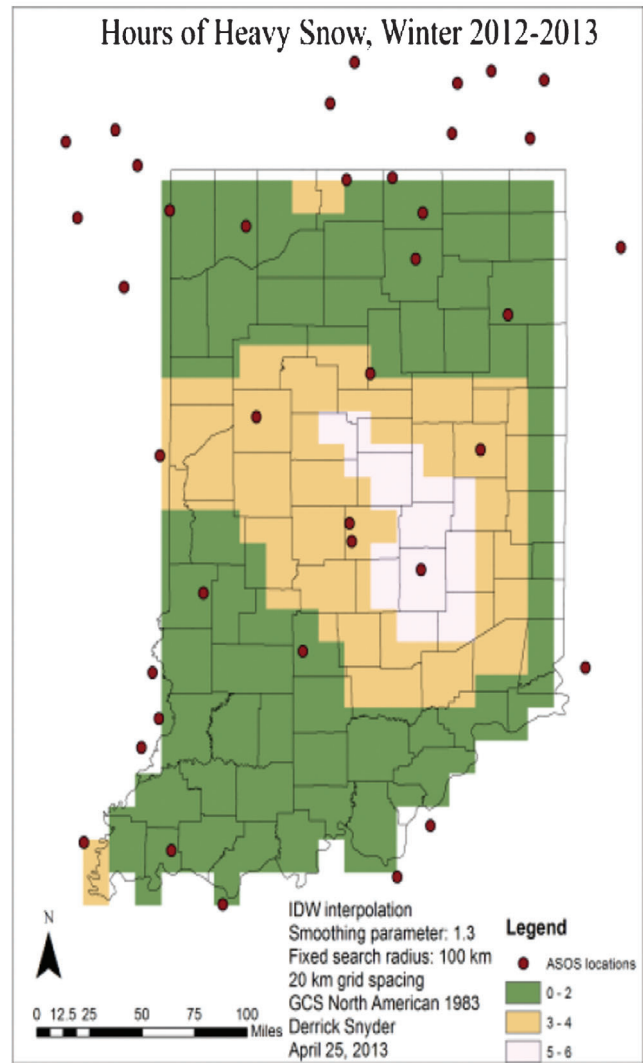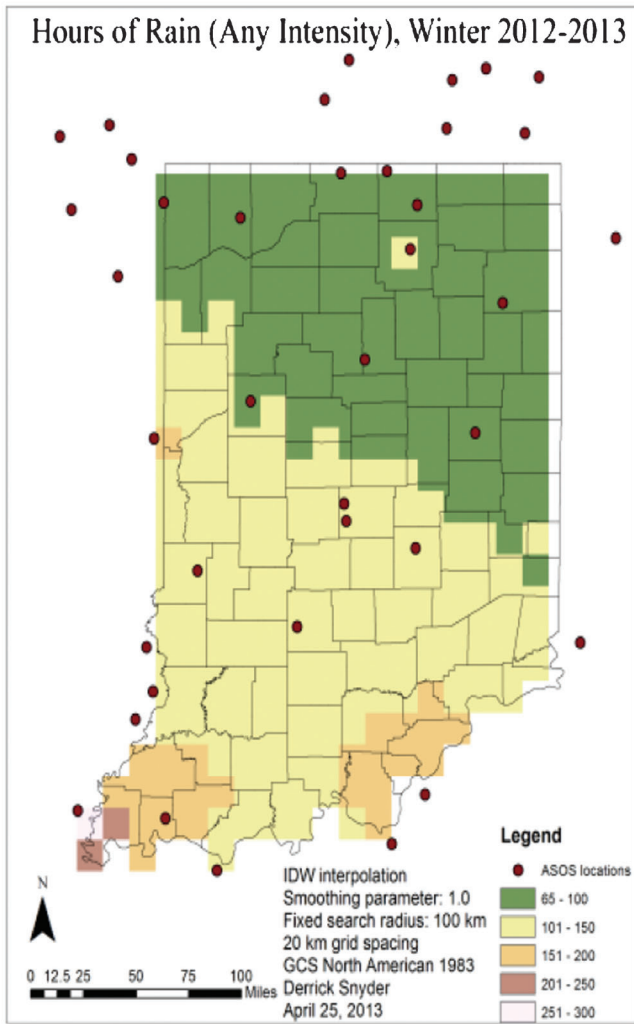
Figure 2.11 "Stage I" observation-based analysis of hours of rain for the 2013 season.

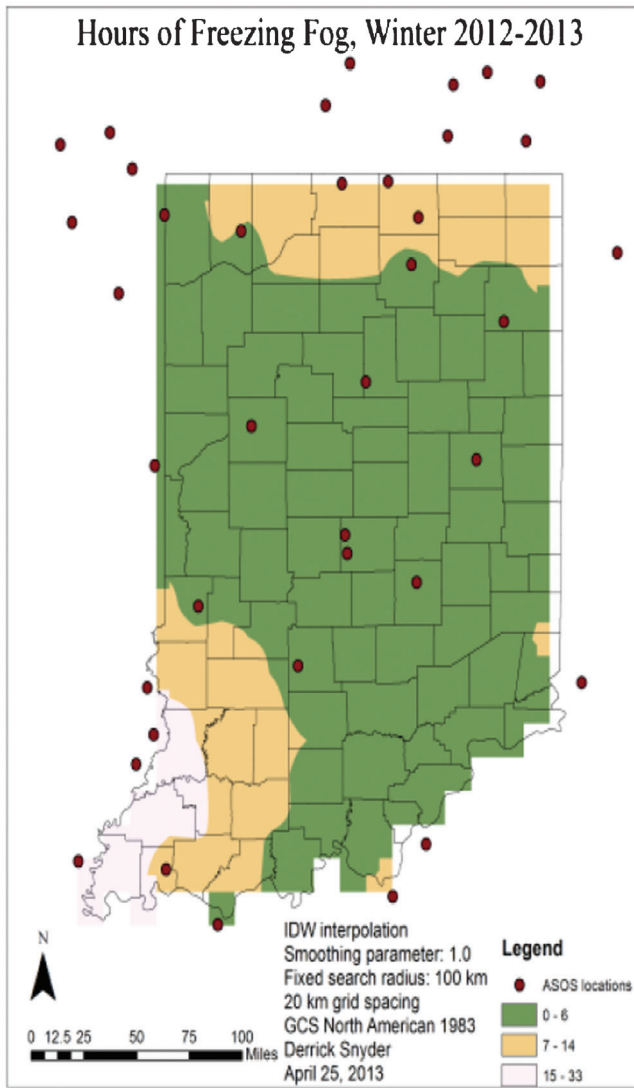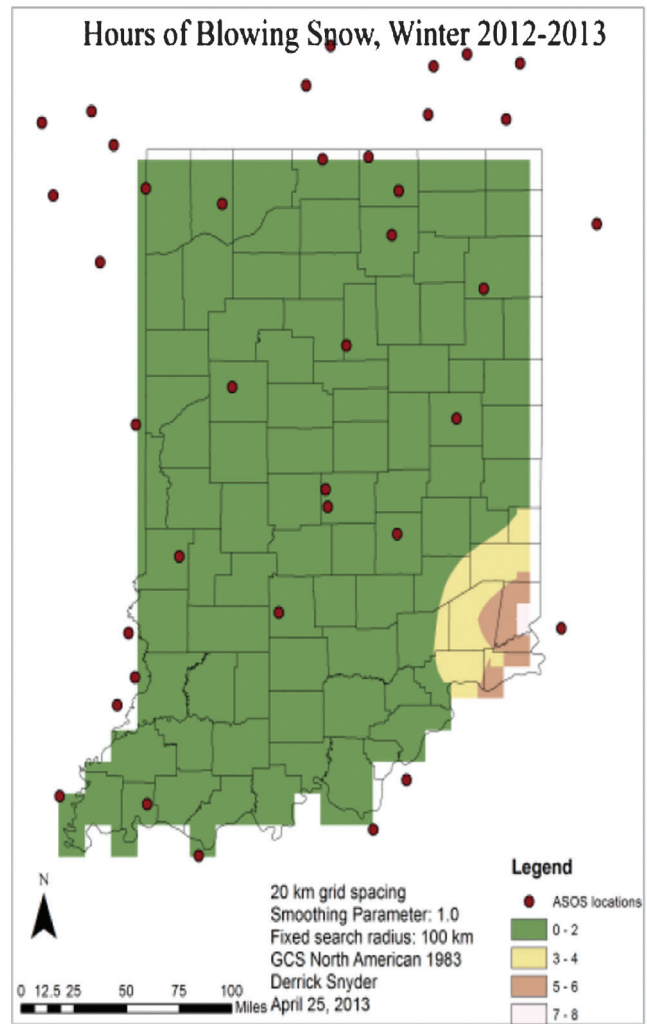**Figure 2.12** "Stage I" observation-based analysis of hours of blowing snow for the 2013 season.

2.2.1.1 Rapid Refresh/Rapid Update Cycle. The Rapid Refresh (RAP) is an hourly, short-range (18 hour forecasts) weather model and data assimilation system was operationally implemented at the National Centers for Environmental Prediction (NCEP) on 1 May 2012. The RAP replaced the previous Rapid Update Cycle (RUC) forecast system. The RAP has a horizontal grid spacing of approximately 13 km with 50 levels in the vertical. Because new forecasts and analyses are available every hour, the RAP lends itself nicely for the use of estimating hourly weather conditions. Contained within the RAP dataset are four categorical precipitation type variables—rain, snow, ice pellets, and freezing—that will be used to estimate winter weather hours. These classifications are based up on a series of logic that involve vertical thermal and moisture profiles and information derived from the cloud microphysics parameterization. However, the classifications are not mutually exclusive; that is, more than one precipitation type designation may exist for the same grid point location. A winter

weather hour was counted if one of these classifications were designated while at the same time the 1-hour forecasted precipitation amount exceeded 0.1 mm. This criterion was introduced in order to account for the high bias of estimated rain and snow hours (compared to other data source estimations) the occasions when the model was not producing a reasonable amount of accumulated precipitation and yet. For example, Figure 2.14a and 2.14b compares the 2012–2013 snow hours with and without the precipitation accumulation threshold, respectively.

For the 2010–2011 season, the 13 km RUC data was not available, and thus the coarser 20 km data was utilized. Seasonal estimates of winter weather hours for the past three winter seasons were compiled by summing the number of occurrences of each precipitation type for each hour between 06Z November 1 and 06Z April 1 where the 1-hour forecast precipitation amount exceeded 0.1 mm. Monthly and daily accumulations were also computed.
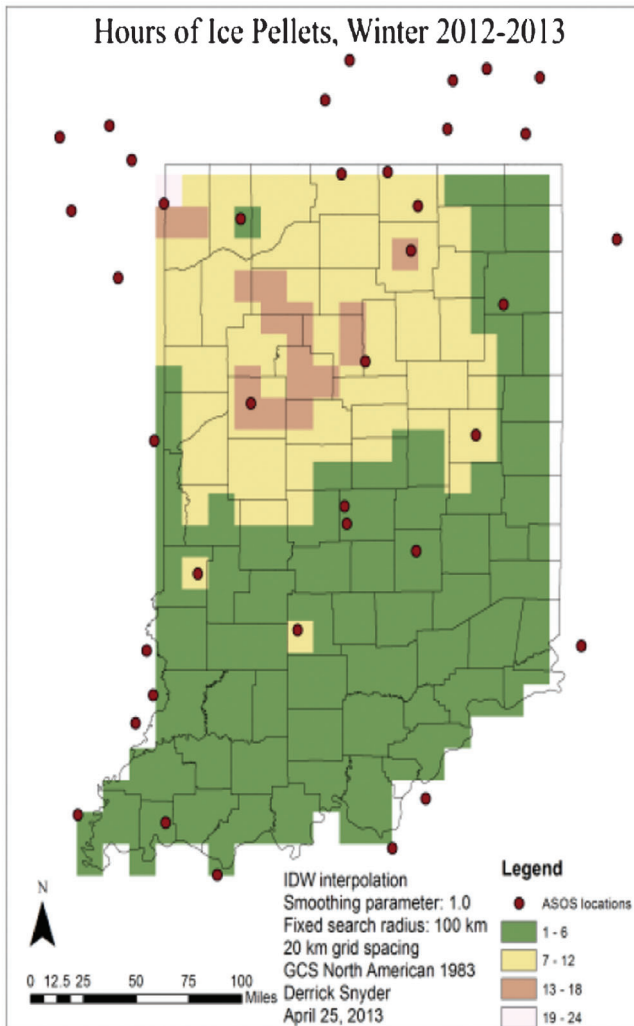
Figure 2.13 "Stage I" observation-based analysis of hours of ice pellets for the 2013 season.

2.2.1.2 Real-Time Mesoscale Analysis (RTMA). The Real-Time Mesoscale Analysis (RTMA) dataset is a high-resolution (~5 km grid spacing) gridded meteorological analysis of sensible weather variables—2 m temperature, 2 m dew point temperature, 2 m specific humidity, 10 m wind, surface pressure, and hourly precipitation estimates (5). RTMA quantitative precipitation estimates (QPE) are obtained from the 4 km gridded NCEP Stage II hourly precipitation estimates interpolated to the 5 km RTMA grid. Stage II QPE utilizes a combination of hourly radar and rain gauge estimated rainfall accumulation to arrive at a multi-sensor precipitation approximation (6).

As categorical precipitation type is not an available variable in this dataset, a different approach to estimate winter weather hours, based solely upon the available meteorological variables, was needed. With only near surface variables available, precipitation type is somewhat trickier to infer, and as a result, only

frozen and liquid precipitation were designated as precipitation types. Frozen precipitation was estimated to occur if:

1. precipitation estimate > 0 mm
2. 2 m temperature $< 2°C$
3. wet-bulb temperature $< 0°C$

Otherwise, if the temperature and wet-bulb temperature criteria were not met, yet there was measurable precipitation, liquid precipitation was recorded. Daily, monthly, and seasonal tabulations were created based upon these criteria.

2.2.1.3 National Mosaic and Multi-Sensor QPE (NMQ) System. Another high-resolution dataset available is the National Mosaic and Multi-Sensor QPE (NMQ) System produced by the National Severe Storms Lab (NSSL). The NMQ system is multi-sensor dataset that ingests information from 170 weather radars, rain gauge data, and RUC/RAP model analysis fields (7). NMQ provides 2D and 3D radar mosaics on a $0.01° \times 0.01°$ latitude/longitude grid (~1 km $\times$ 1 km). Data incorporated from rain gauges and model analyses allow for the NMQ system to provide products regarding precipitation estimates and precipitation type classification. In regard to the task at hand, the primary focus was upon the gridded precipitation type product. The five precipitation types identified by NMQ— stratiform rain, convective rain, warm rain, hail, and snow—are derived from a series of logic based upon thermal and moisture variables obtained from the RUC/RAP analyses. Snow is the determined precipitation type if the hybrid scan reflectivity (i.e., the reflectivity values of the lowest radar elevation scan):

1. < 5 dBZ and surface temperature $< 2°C$
2. < 10 dBZ, surface temperature $< 2°C$, and surface wet-bulb temperature $< 0°C$.

Daily, monthly, and seasonal tabulations were created using this snow designation from hourly NMQ data, but only for the 2012–2013 season at this time.

2.2.2 Missing Data

The total number of hours possible for the 2010–2011 and 2012–2013 seasons was 3625 hours each, but because 2012 was a leap year, the total possible hours was 3649. Unfortunately, a number of hourly data files were missing for each season and across each of the three datasets as shown in Table 2.4. Ultimately, the data for the 2012–2013 was the most reliable with the fewest number of missing files. For both RAP/RUC and RTMA, the number of missing files from the NCDC archive increased markedly for each past season. As a result, estimates for these seasons may not be truly representative. A list of the dates that are missing files for each data set in each season may be found in Appendix A.

a)

b)
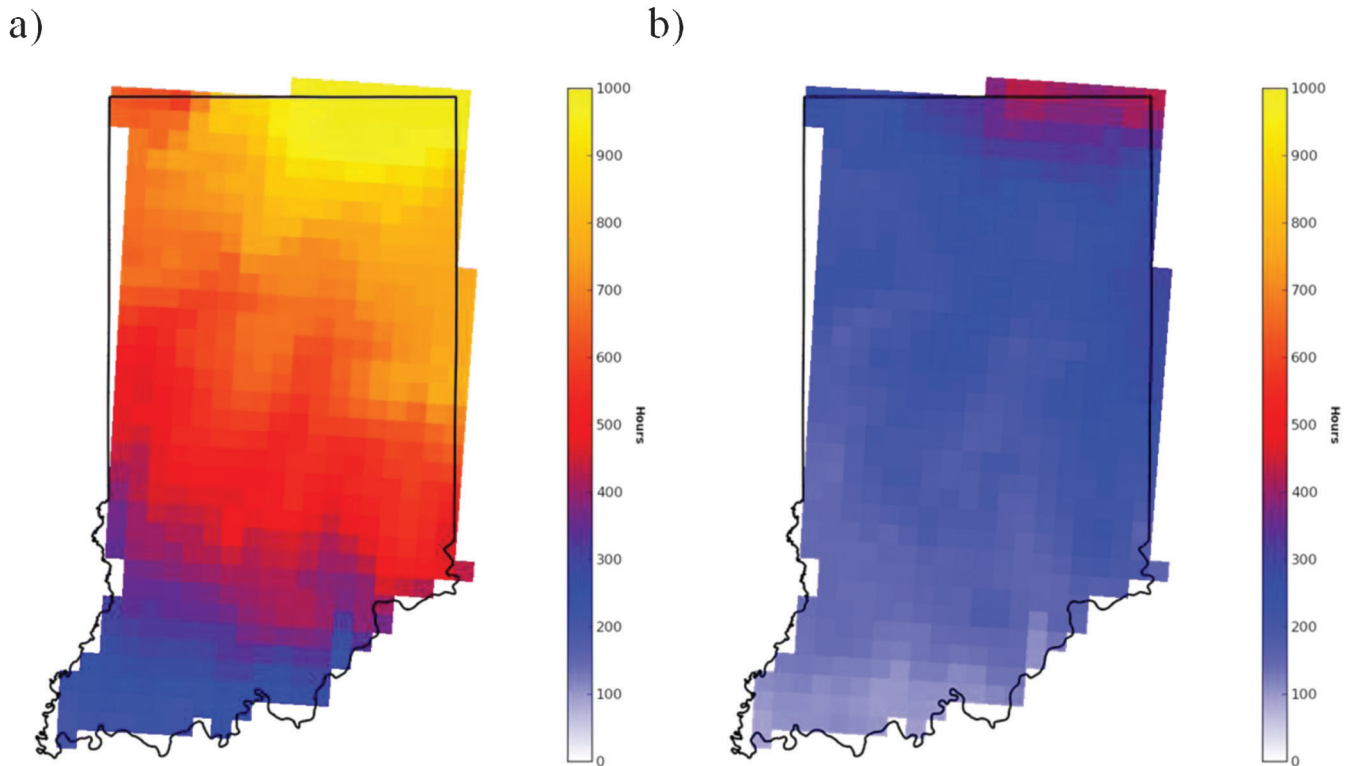
Figure 2.14 RAP accumulated snow hours for 2012–2013 (a) without precipitation threshold and (b) with precipitation threshold.

2.2.2.1 Web Portal. Images for daily, monthly, and seasonal totals are available for viewing through a web interface at the following URLs:

1. Daily: http://weather.eaps.purdue.edu/cgi-bin/daily_winter_wx_hours.py
2. Monthly: http://weather.eaps.purdue.edu/cgi-bin/monthly_winter_wx_hours.py
3. Seasonal: http://weather.eaps.purdue.edu/cgi-bin/season_winter_wx_hours.py

2.3 "Stage III" Estimates of Winter Weather Hours for the 2013 Season

The National Weather Service Weather Surveillance Radar-1988 Doppler (WSR-88D) radar network recently completed an upgrade to dual-polarimetric technology. Dual-polarization radar, hereafter referred to as "dual-pol," unlike the conventional WSR-88D radars that emit only horizontally oriented pulses, transmit both horizontally and vertically oriented

pulses. As such, dual-pol radar provides an advantage over conventional single polarization radar in that it can provide more useful information about targets, in particular the size, shape, and concentration of which may be used to deduce hydrometeor type. In addition, it may also aid in the discrimination between meteorological and non-meteorological targets. There are three dual-pol variables available in the raw level II data: differential reflectivity (Z_{DR}), correlation coefficient (ρ_{HV}), and differential propagation phase shift (Φ_{DP}).

Differential reflectivity is simply the ratio between the linear reflectivity factor (z) returned for both the horizontal (z_H) and vertical (z_V) polarized signals, or when Z_H and Z_V are in logarithmic units (that is, measured in units of dBZ rather than $mm^6\ m^{-1}$), then Z_{DR} (in units of dB) is simply the difference between Z_H and Z_V (*8*). Differential reflectivity depends upon the aspect ratio of the targets, and therefore can offer information regarding shape of hydrometeors.

Correlation coefficient is a measure of the correlation between the horizontal and vertical polarized signals. This variable can also be a good discriminator between meteorological and non-meteorological scatterers. For example, where ρ_{HV} is less than 0.8, the horizontal and vertical oriented pulse returns behave differently from pulse to pulse and likely are representative of complex scattering due to non-meteorological targets such as birds and insects. Another dual-polarization variable is the total differential phase shift (Φ_{DP}), often referred to

TABLE 2.4
Number of missing data files (hours) for each season

Data Source	2010–2011	2011–2012	2012–2013
RAP/RUC	233	115	8
RTMA	115	48	5
NMQ	N/A	N/A	15

simply as differential phase. Differential phase relates the phase shift between the horizontally and vertically oriented beams as they travel through some medium, typically hydrometeors. The magnitude of Φ_{DP}, measured in degrees, depends upon several factors such as hydrometeor size, concentration, and orientation (8); because of these differences, phase shifting may not occur equally for the horizontal and vertical beam pulses.

Differential phase is a range cumulative quantity (9), and therefore depends upon the distance from the radar. As a result, Φ_{DP} in itself is difficult to interpret and thus is not that useful of a product (8). Rather, the range derivative of the Φ_{DP} profile may be taken to determine the meteorologically significant areas where the phase shifting is occurring. This derived quantity is termed the specific differential phase (K_{DP}) is meant to isolate where in the Φ_{DP} profile the phase shifting occurs, and it is a more useful product, particularly in the estimation of rainfall rates.

From these variables, several algorithms have been developed for the purpose of providing improved estimates of precipitation rates and precipitation type classification. The purpose of this task was to utilize the information provided by dual-pol radar to provide winter weather hour estimates for the 2012–2013 season. Efforts to accomplish this are underway, and the following will describe the work that has been done thus far toward this goal.

2.3.1 Data Format and Visualization

Level II radar data is compressed and received in MSG31 binary data format in near real-time at Purdue via Unidata's Local Data Manager (LDM) software. Archived radar data may be obtained from the National Climatic Data Center (NCDC). The transition from MSG1 to MSG31 format was necessitated by the need to include Super Resolution ($0.5° \times 0.25$ km) (10) and dual-polarization data in the real-time Level II distribution of data. The radar data was converted from MSG31 format to Network Common Data Format (NetCDF) CF-radial format using the NetCDF-Java library (Unidata; http://www.unidata.ucar.edu/software/netcdf-java/). Data within the file are stored in the native radar coordinate system; a local spherical coordinate system represented by the radial azimuth(α), elevation angle (θ_e), and range distance (r) with respect to the radar's central location.

The simplest means by which to visualize radar data involves a spherical to Cartesian coordinate transformation. However, the process of plotting radar data upon a map is not as straightforward, however. In order to do so, each radial range gate must be geo-referenced with a corresponding latitude and longitude. To accomplish this task, first each location will need to have a corresponding ground distance and height above ground level variable. These values are computed from the native radial distance and elevation values in addition to the latitude and altitude of the radar location.

Following (11), the radial radar beams are assumed to follow the 4/3 effective earth radius model:

$$h = \left[r^2 + (k_\theta a)^2 + 2rk_\theta a \sin \theta_\theta \right]^{\frac{1}{2}} - k_\theta a + H_0 \qquad (1)$$

$$s = k_\theta a \sin^{-1} \left(\frac{r cos\theta_\theta}{k_\theta a + h} \right) \qquad (2)$$

$$k_\theta a \approx \frac{4}{3} a \qquad (3)$$

where h is the height above ground level, s is ground distance, a is the equatorial radius of the earth ($\sim$6370 km), r is the radial distance, H_0 is the height of the radar platform.

With this information, the Vincenty formula (12) for a direct geodetic transform may be used to find the latitude and longitude coordinate for each radial gate location in each sweep. In this application of the Vincenty formula, all that is needed to calculate the latitude and longitude of each gate is the latitude and longitude of the origin (i.e., radar location), the azimuth angle, and the ground distance. The full iterative formula is presented in Appendix B.

2.3.2 Example: 5–6 March 2013

As aforementioned, several algorithms have been developed for the purpose of providing improved estimates of precipitation rates and precipitation type classification, many of which are available as Level-III radar products. This section will focus upon the performance of the hydrometeor classification algorithm (HCA), an algorithm that uses fuzzy logic to classify radar echoes into ten separate categories based upon information from dual-pol variables (13). The ten classes are as follows: ground clutter/anomalous propagation, biological scatterers, dry aggregated snow, wet snow, ice crystals, Graupel, "big drops," light/moderate rain, heavy rain, rain/hail. To evaluate HCA, surface observations and reports from the Meteorological Phenomena Identification Near the Ground (mPING) project will serve as the best estimate of ground "truth." mPING allows for the public to report weather information, such as precipitation type, via a smart phone application. Options for precipitation type include: none, drizzle, freezing drizzle, rain, freezing rain, ice pellets/sleet, snow, mixed rain and snow, mixed rain and ice pellets, mixed ice pellets and snow, and hail. While these categories do not line up with the HCA classifications, they can at least provide insight as to whether frozen or liquid precipitation is occurring at the surface.

The storm of 5–6 March 2013 produced several different precipitation types across central and northern Indiana, therefore serving as an excellent case to examine the ability of the HCA algorithm to classify winter precipitation. At 12 UTC 5 March, scattered light rain showers are found northern Indiana, but by afternoon began to transition to a wintry mix of ice pellets and sleet, from south to north, before changing

over to all snow by 22Z. By 12Z the next day, 5–6 inches of wet snow had fallen across central Indiana with higher amounts of 8–10 inches further north. A 24 hour animation of Indianapolis radar variables, from the period 12Z 5 March to 12Z 6 March, may be viewed in the following links:

- Base reflectivity (super-resolution): http://weather.eaps. purdue.edu/INDOT/mar_5_6/superres_loop.html
- Differential reflectivity: http://weather.eaps.purdue.edu/ INDOT/mar_5_6/zdr_loop.html
- Correlation coefficient: http://weather.eaps.purdue.edu/ INDOT/mar_5_6/cc_loop.html
- Specific differential phase: http://weather.eaps.purdue. edu/INDOT/mar_5_6/kdp_loop.html
- Hydrometeor Classification Algorithm: http://weather. eaps.purdue.edu/INDOT/mar_5_6/hca_loop.html

For the sake of brevity, much of the discussion will revolve around the performance of the HCA product. The concentric light green circle around the radar location (designated as light/moderate rain) present on many occasions in the HCA images is due to the fact that the current HCA algorithm does not account for refreezing of hydrometeors below the melting level, a major shortcoming of the algorithm (14). Precipitation can refreeze below the melting layer and also very near or at the surface (e.g. freezing rain). For example, Figure 2.15b shows the HCA classification with mPING reports valid within the last 15 minutes for 2147Z on 5 March 2013 with the corresponding base reflectivity in Figure 2.15a. As can be seen, the light green circle depicts light to moderate rain, and yet mPING reports show numerous reports of wet snow, snow, and a rain/snow mix in the same areas. In these scenarios where precipitation refreezes below the melting layer, (14) notes that the HCA algorithm will

most "certainly fail" and is not a good candidate, in its current form, to aid in precipitation type classification near the surface. As a result, the best course of action would be to combine radar data with environmental data, perhaps vertical profiles of thermal and moisture information from RAP analyses, to improve precipitation type classification.

2.3.3 Work Plan for Developing Radar-Based Estimate of Winter Weather Hours for 2012–2013

To complete the task as outlined in the work plan, in order to estimate winter weather hours from dual-pol radar data, the next major step will be to transform the data on to a regular latitude/longitude Cartesian grid, similar to that of the NMQ data. As a result, aggregations based upon standard grids will be much more straightforward. The next hurdle will revolve around obtaining the large amount of Level-II data for the entire season.

2.4 Evaluation of Stage I–III Winter Weather Hours

With the completion of Stage I–III winter weather analyses, a comparison of winter weather hour estimates may now be performed in order to evaluate their ability to accurately represent the occurrence of winter precipitation, snow in particular. At this time, we have not yet pursued the question of whether these estimates were able to more precisely define the costs associated with road treatment for winter weather operations, though this effort will be forthcoming. An inter-comparison of estimates for seasonal, monthly, and daily estimates of snow hours from each data set will now be discussed.
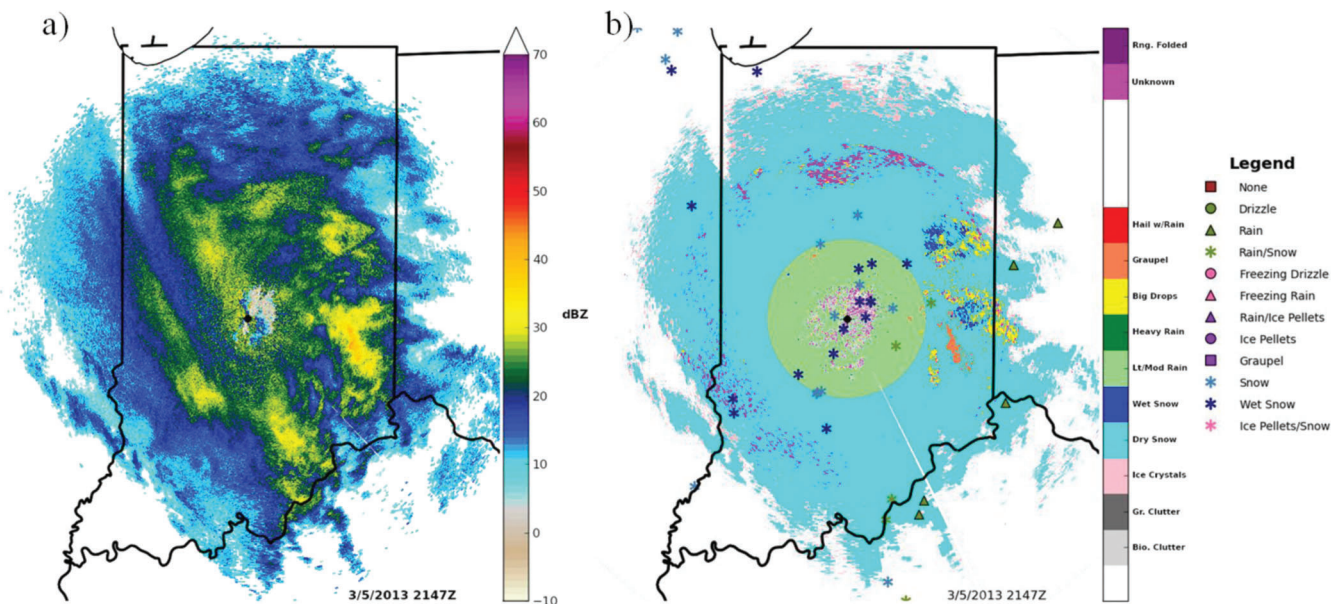
Figure 2.15 Indianapolis (KIND) (a) base reflectivity and (b) HCA with mPING reports data for 2147Z 5 March 2013.

2.4.1 Seasonal

2.4.1.1 2012–2013 Winter Season. Seasonal estimates of winter weather hours, an inter-comparison of results from the 2012–2013 winter season will be discussed. Figure 16a–d illustrates estimates of snow hours from NMQ, RAP, RTMA, and Stage I, respectively. A cursory examination would suggest that the NMQ results closely resemble those of the Stage I estimates, both spatially and in magnitude, with enhanced snow hours in and around the Indianapolis metropolitan area and in the northeast quadrant of the state. The estimates based on RAP somewhat concur with NMQ and Stage I, at least in the sense that it also depicts an increase in snow hours from southwest to northeast. Estimates using RTMA data appear as an outlier, however. All
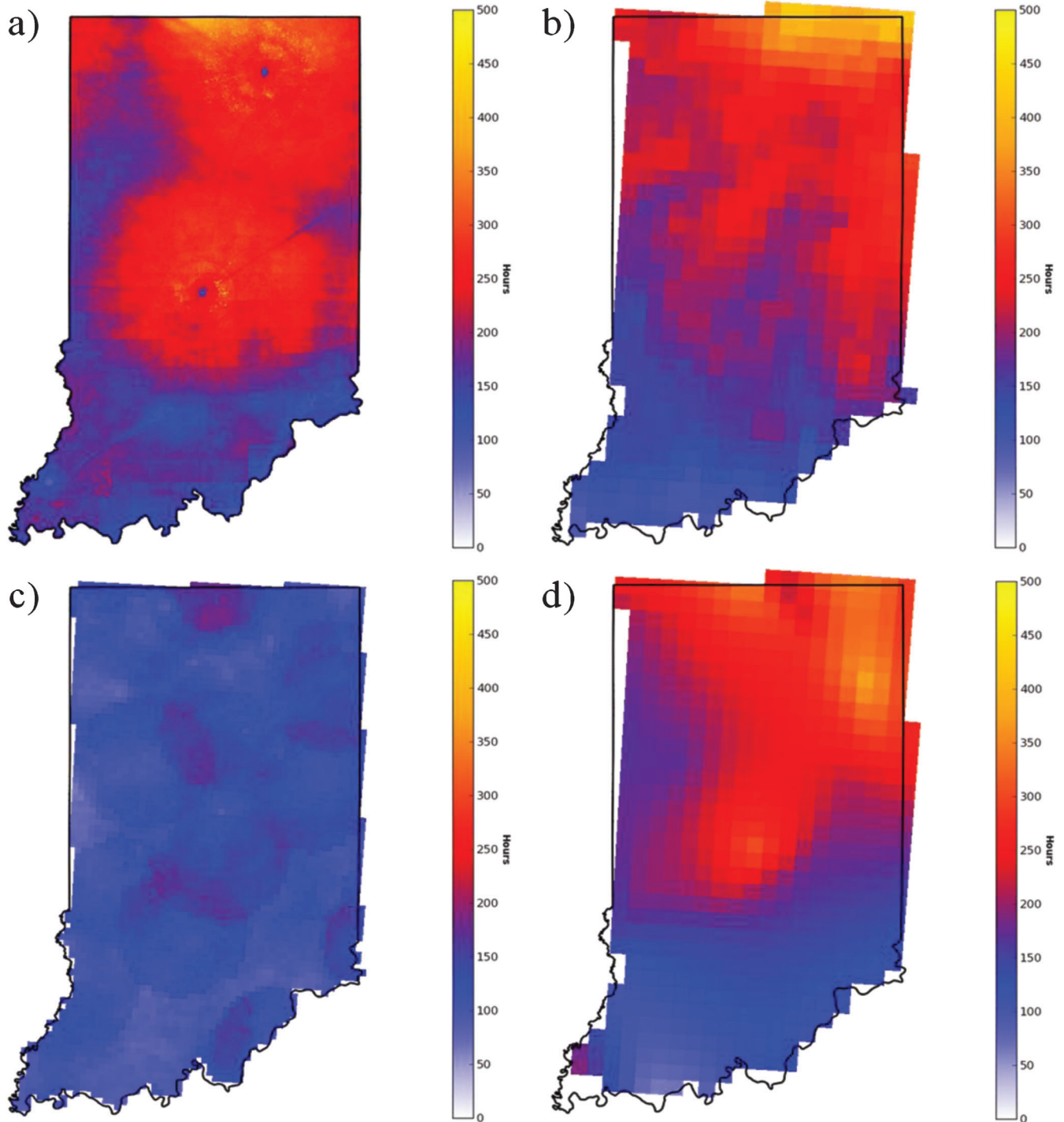
Figure 2.16 Seasonal snow hour estimates for 2012–2013 as estimated by (a) NMQ (b) RAP (c) RTMA and (d) Stage I.

datasets seem to depict an enhanced occurrence of snow hours in the northern tier of Indiana counties, particularly in the South Bend, IN region presumably due to the occurrence of lake-effect snowfall.

To produce a more useful map to highlight spatial differences, we interpolated the Stage I ASOS observations onto the native grid of each dataset using a Delaunay triangulation. This allows for the one-to-one difference maps to be generated. Results of this differencing (Stage I minus the results from the respective data set) are shown in Figure 2.17a–c.

Looking at the data more quantitatively, we are reaffirmed that NMQ and RAP appear to be the most similar in their estimates of seasonal snow hours. For example, the range of values (from minimum to maximum), mean, median, and standard deviation of Indiana snow weather hours for each data set listed in Table 2.5. From these values, we can deduce that NMQ and RAP seem to display magnitude of snow hours that are most comparable, even though from a visual sense the NMQ and Stage I estimate appear most similar in terms of spatial distribution.
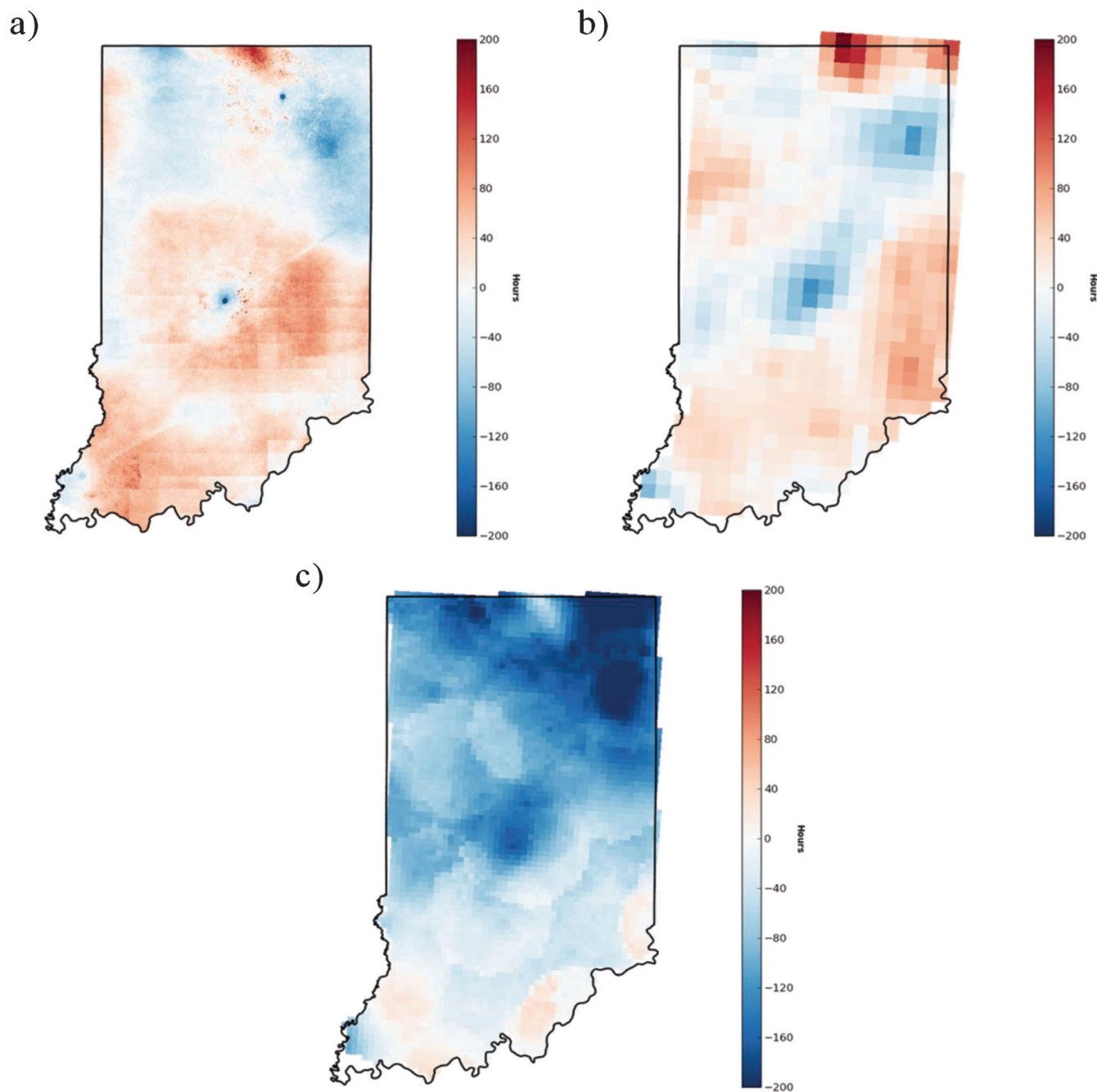
Figure 2.17 Seasonal difference between ASOS observations (interpolated on to native grid using Delaunay triangulation) and estimates from (a) NMQ (b) RAP and (c) RTMA.

TABLE 2.5
Range, mean, median, and standard deviation of estimated snow hours for Indiana's 2012–2013 winter season for each dataset

Data	Range	Mean	Median	Std. Dev.
NMQ	83–481	213.88	216	51.91
RAP	90–426	208.81	206	62.47
RTMA	64–186	119.59	118	20.59
Stage I (ASOS)	65–369	200.59	196	66.08

Figure 2.18 RTMA accumulated precipitation (mm) for the 2012–2013 season.

It is clearly evident from both a qualitative and quantitative perspective that RTMA estimates are certainly under-estimating the occurrence of estimated snow hours as compared to the other data sets. It was determined that this outcome was not the result of the RTMA methodology per se, but rather that the RTMA weather hours are heavily dependent upon the multi-sensor NCEP Stage II precipitation estimates. As can be seen, the circular patterns evident in Figure 2.16c visibly correspond to the overall seasonal estimation of precipitation (mm) shown in Figure 2.18. These circular patterns can be found in the original NCEP Stage II precipitation analyses, likely an artifact of the merging of rain gauge data with radar-based precipitation estimates. A constant radius of influence can be seen in the NCEP Stage II precipitation analyses in the vicinity of isolate rain gauge reports.

Table 2.6 depicts the estimated number of snow hours for each station location based upon the actual raw station observations and the closest grid point to that location for each of the data sets. Also shown, in parentheses, are the deviations of the point location estimates compared to the raw station observation estimates. Undoubtedly, the Stage I estimates most closely align with the actual station observation estimates, as Stage I estimates are interpolated from these observations. NMQ overestimates the occurrence of snow hours for most station locations, with the

exception for Indianapolis (KIND), Terre Haute (KHUF), and Fort Wayne (KFWA). A likely explanation for the significant underestimation at KIND is the collocation of the observation site and the radar site. As noticeable in Figure 2.16a, in the location of the radar sites, a small circular location illustrates small values of snow hours compared to the areas surrounding it. This is a result of the radar's "cone of silence," essentially the diameter around the radar which cannot be sampled by

TABLE 2.6
Comparison of snow weather hours between raw station observations and the closest grid point in NMQ, RAP, RTMA, and Stage I estimates*

Station	Station Obs.	NMQ	RAP	RTMA	Stage I
West Lafayette (KLAF)	171	209 (+38)	186 (+15)	98 (−73)	171(0)
Indianapolis (KIND)	313	137*/248 (−176/−65)	181 (−132)	136 (−177)	302 (−11)
Terre Haute (KHUF)	197	182 (−15)	142 (−55)	102 (−95)	188 (−9)
Fort Wayne (KFWA)	377	244 (−133)	254 (−123)	133 (−244)	369 (−8)
South Bend (KSBN)	353	382 (+29)	326 (−27)	172 (−181)	330 (−23)
Evansville (KEVV)	113	162 (+49)	104 (−9)	107 (−6)	102 (−11)
Bloomington (KBMG)	152	207 (+55)	191 (+39)	117 (−35)	149 (−3)
Muncie (KMIE)	210	215 (+5)	206 (−4)	114 (−96)	214 (+4)

*Shown in parentheses are the deviations (+/−) from the corresponding station observation values.

NOTE: The KIND location falls within the radar's "cone of silence," and as evidenced by Figure 2.16a, the area surrounding the radar location depicts reduced estimates of snow hours. By moving 0.1° longitude further to the west (along the same parallel), a marked increase in the snow hour estimate is seen (shown after slash).
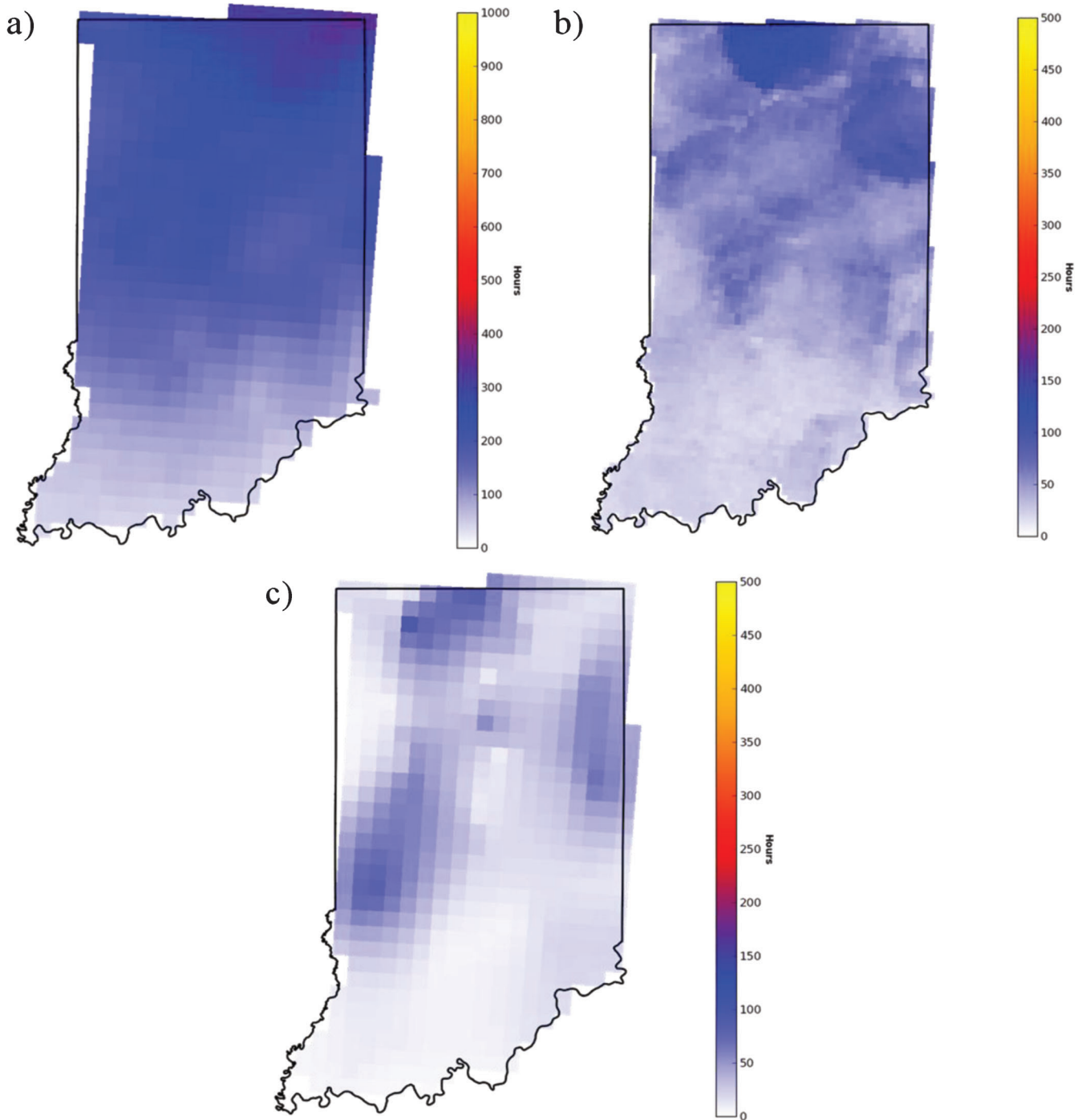
Figure 2.19 Seasonal snow hour estimates for 2011–2012 as estimated by (a) RUC (b) RTMA and (c) Stage I.

the radar beam. This result is not surprising, as NMQ precipitation type is based upon the available radar data. By shifting 0.1° further west in longitude, the NMQ estimate increases from 137 to 248 hours; this is still lower than the observation site estimate, however the gap between the two measures has been reduced significantly.

Once again, these data confirm that RTMA is underestimating the number of observed snow hours, particularly in central and northeastern Indiana.

2.4.1.2 2011–2012 Winter Season. See Figures 2.19 and 2.20 for the 2011–2012 winter season totals.

2.4.1.3 2010–2011 Winter Season. See Figures 2.21 and 2.22 for the 2010–2011 winter season totals.

2.4.2 Monthly

See Figures 2.23 through 2.27 for the monthly totals for 2012–2013.
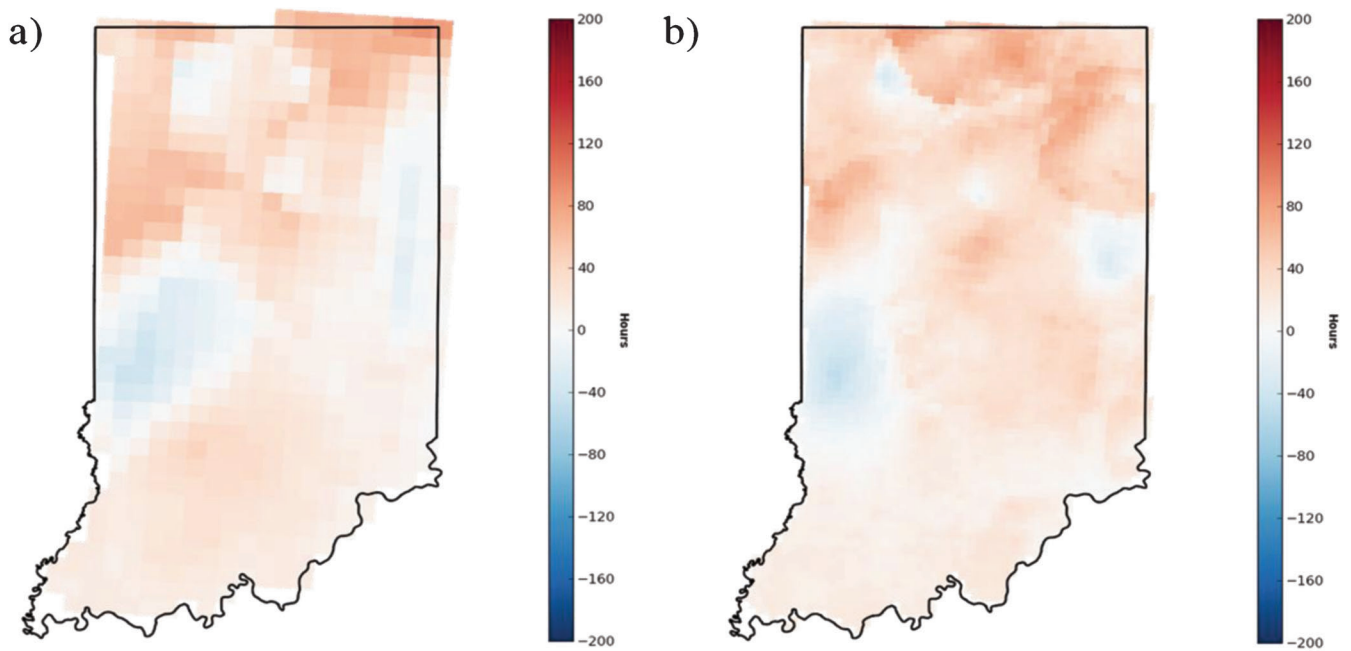
Figure 2.20 Seasonal difference between ASOS observations (interpolated on to native grid using Delaunay triangulation) estimates from (a) RUC and (b) RTMA.
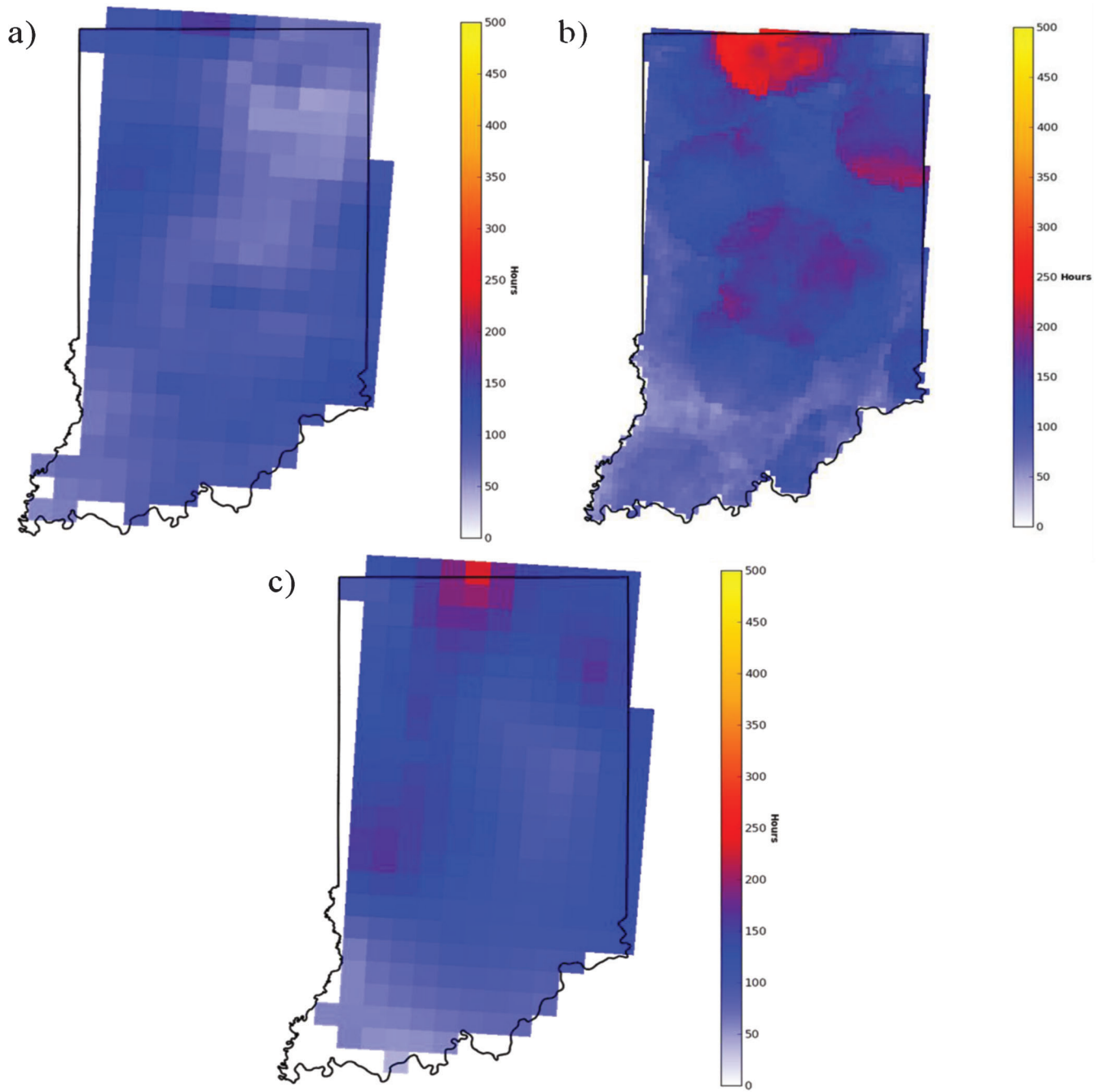
Figure 2.21 Seasonal snow hour estimates for 2010–2011 as estimated by (a) RAP (b) RTMA and (c) Stage I.
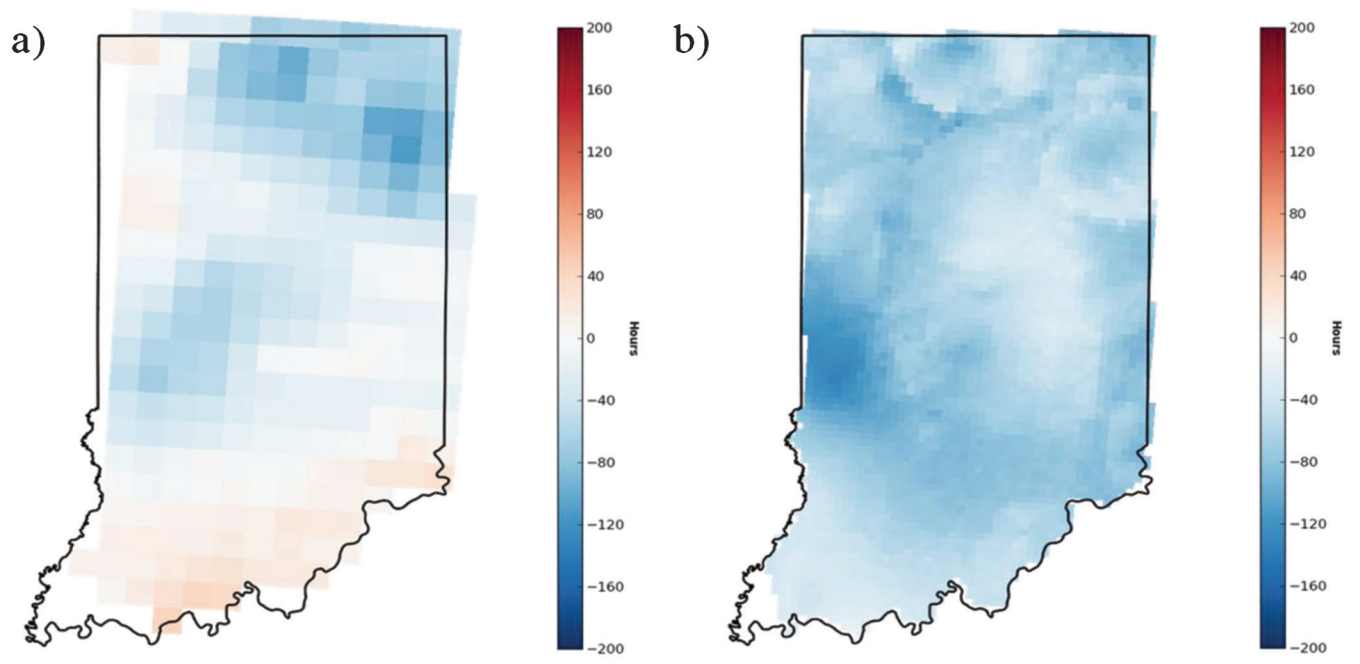
Figure 2.22 Seasonal difference between ASOS observations (interpolated on to native grid using Delaunay triangulation) estimates from (a) RUC and (b) RTMA.
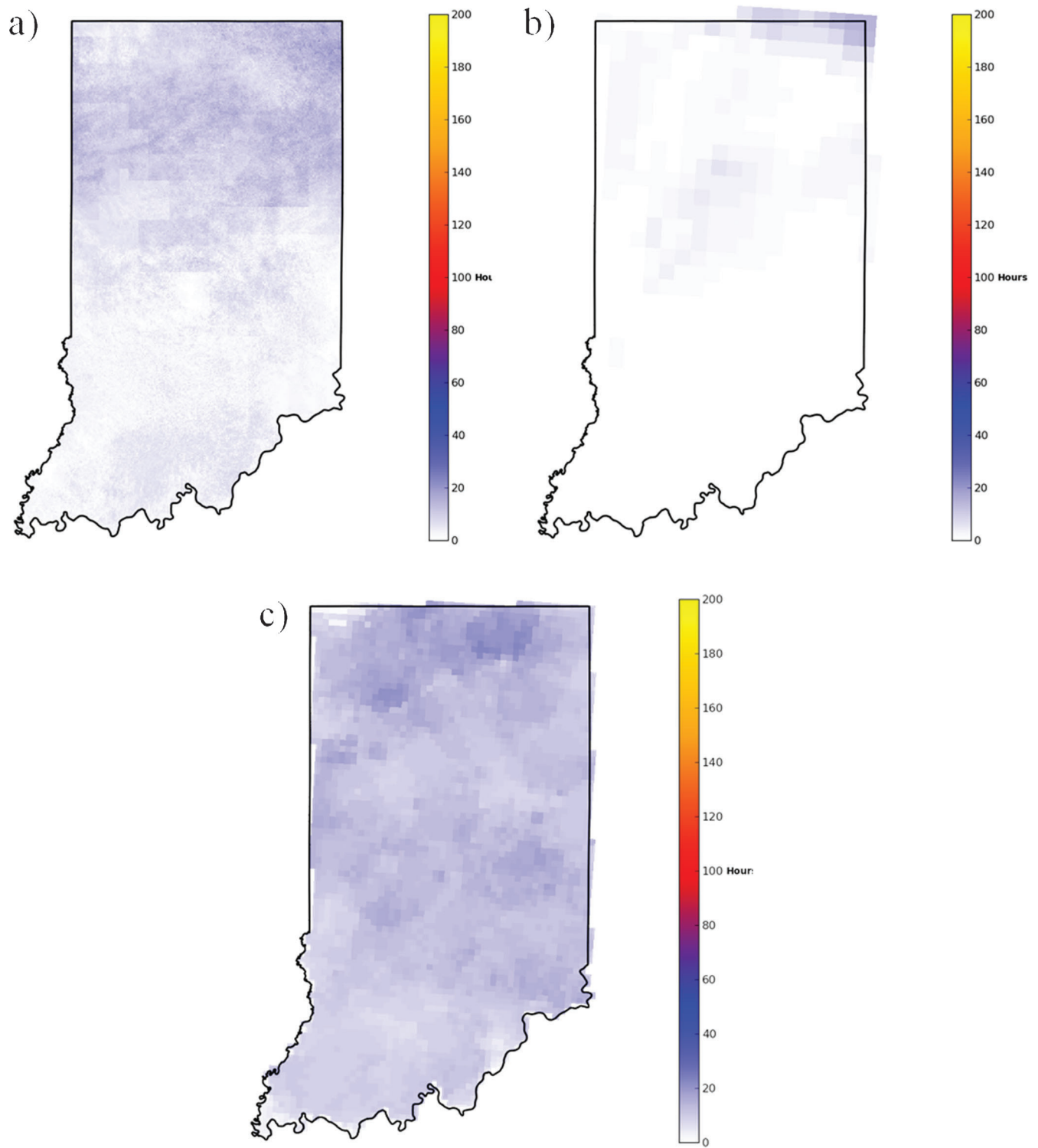
Figure 2.23 November monthly snow hour estimates for 2012–2013 as estimated by (a) NMQ (b) RAP (c) RTMA.
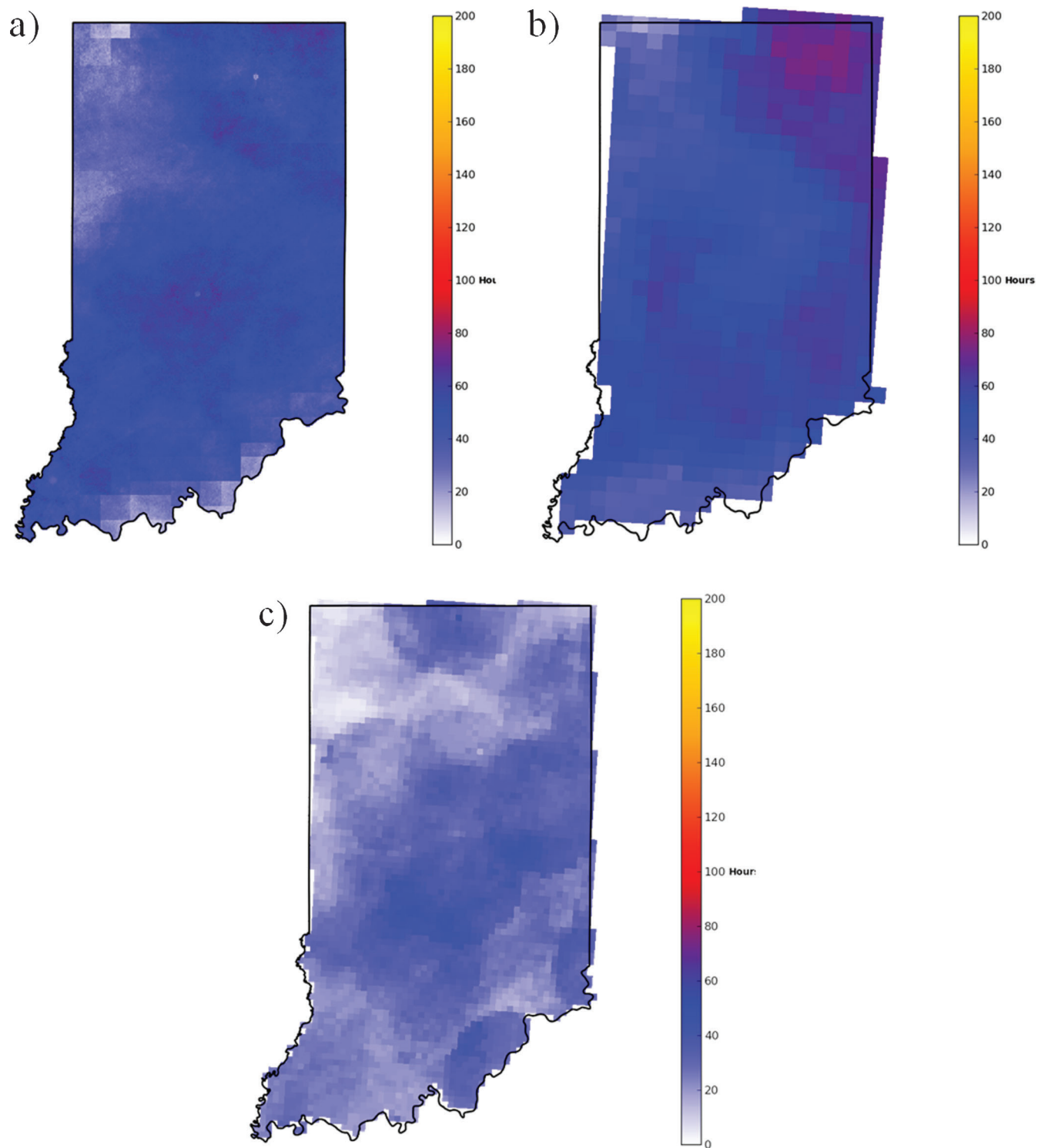
Figure 2.24 December monthly snow hour estimates for 2012–2013 as estimated by (a) NMQ (b) RAP (c) RTMA.
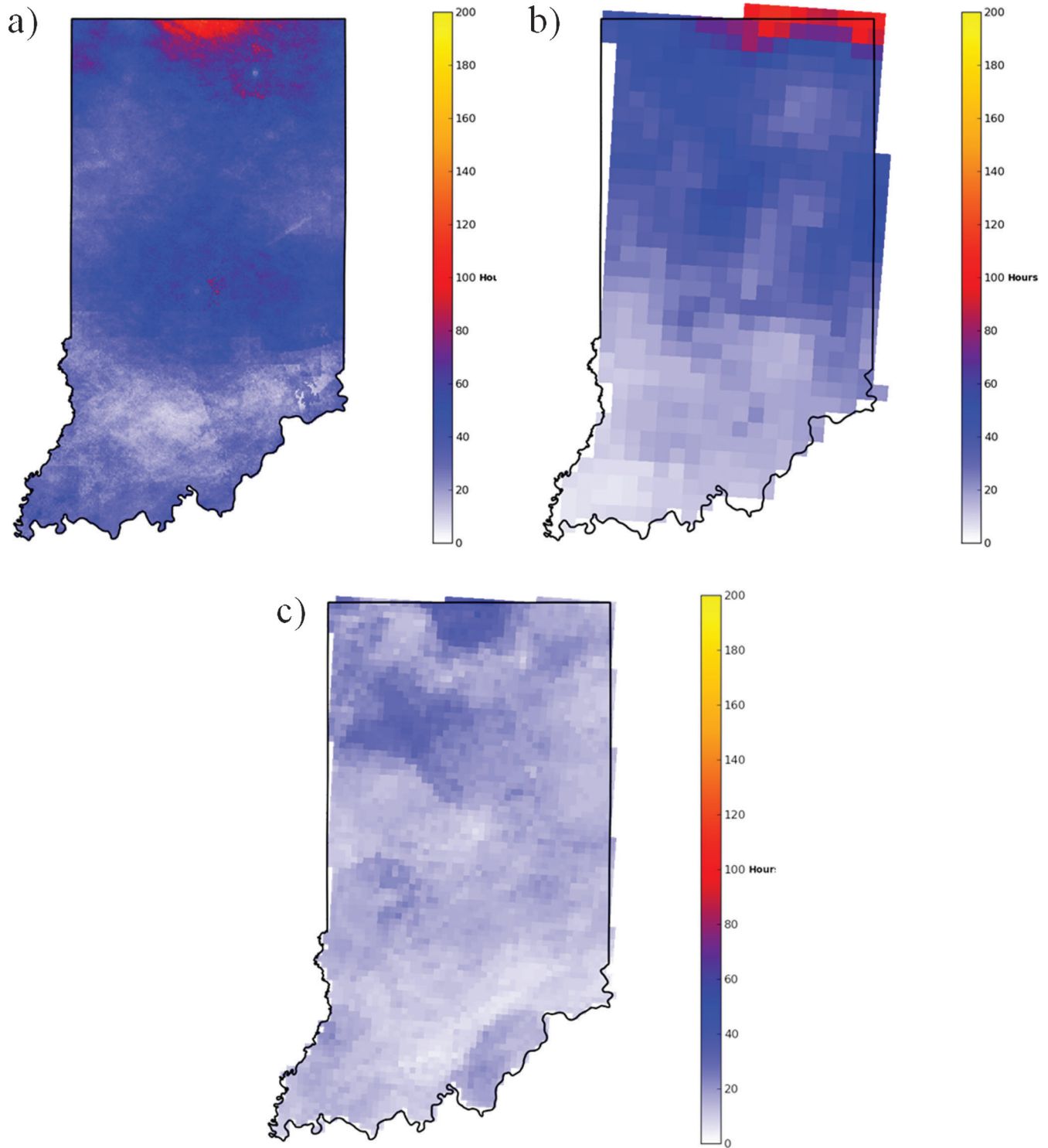
Figure 2.25 January monthly snow hour estimates for 2012–2013 as estimated by (a) NMQ (b) RAP (c) RTMA.
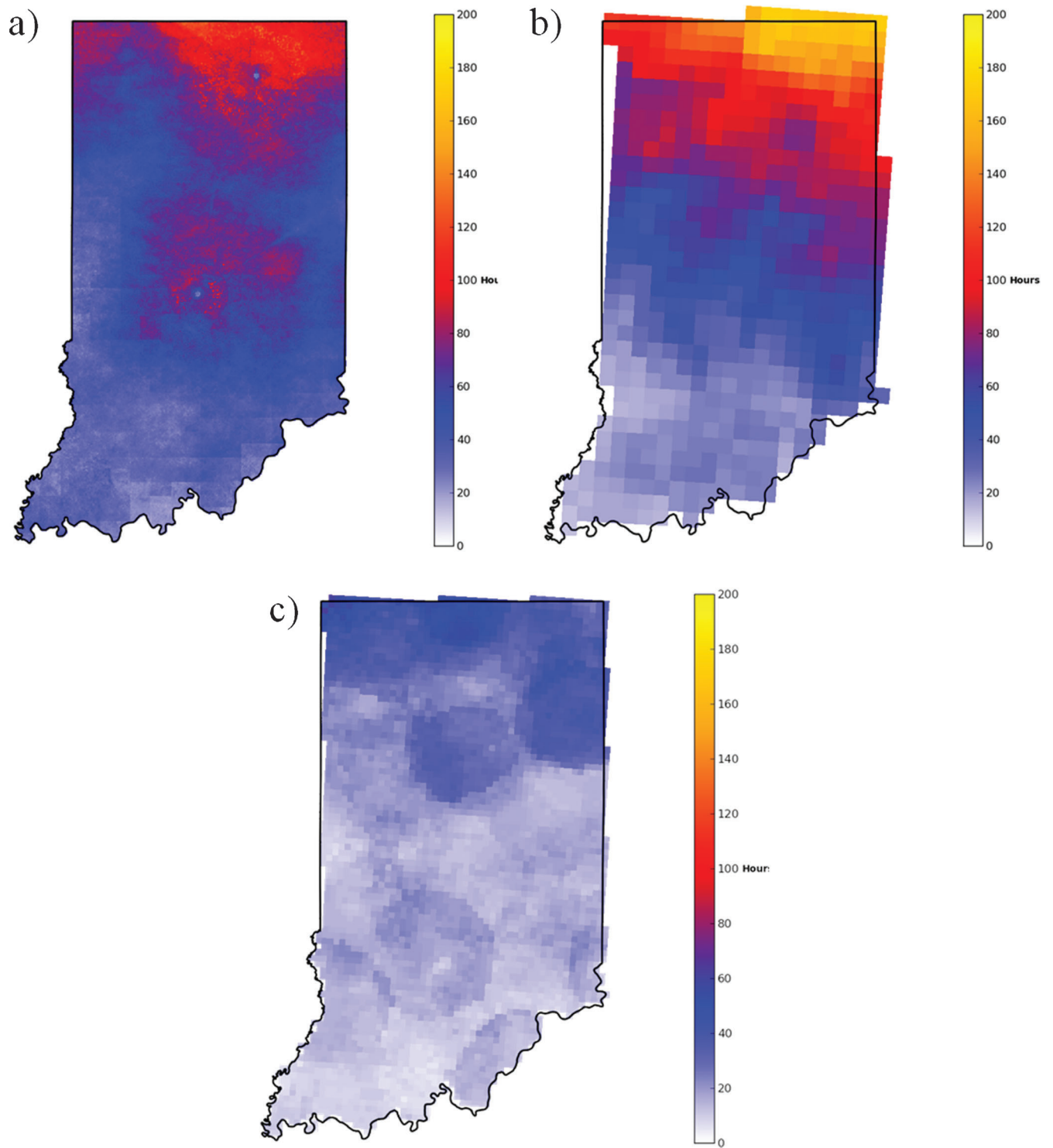
Figure 2.26 February monthly snow hour estimates for 2012–2013 as estimated by (a) NMQ (b) RAP (c) RTMA.
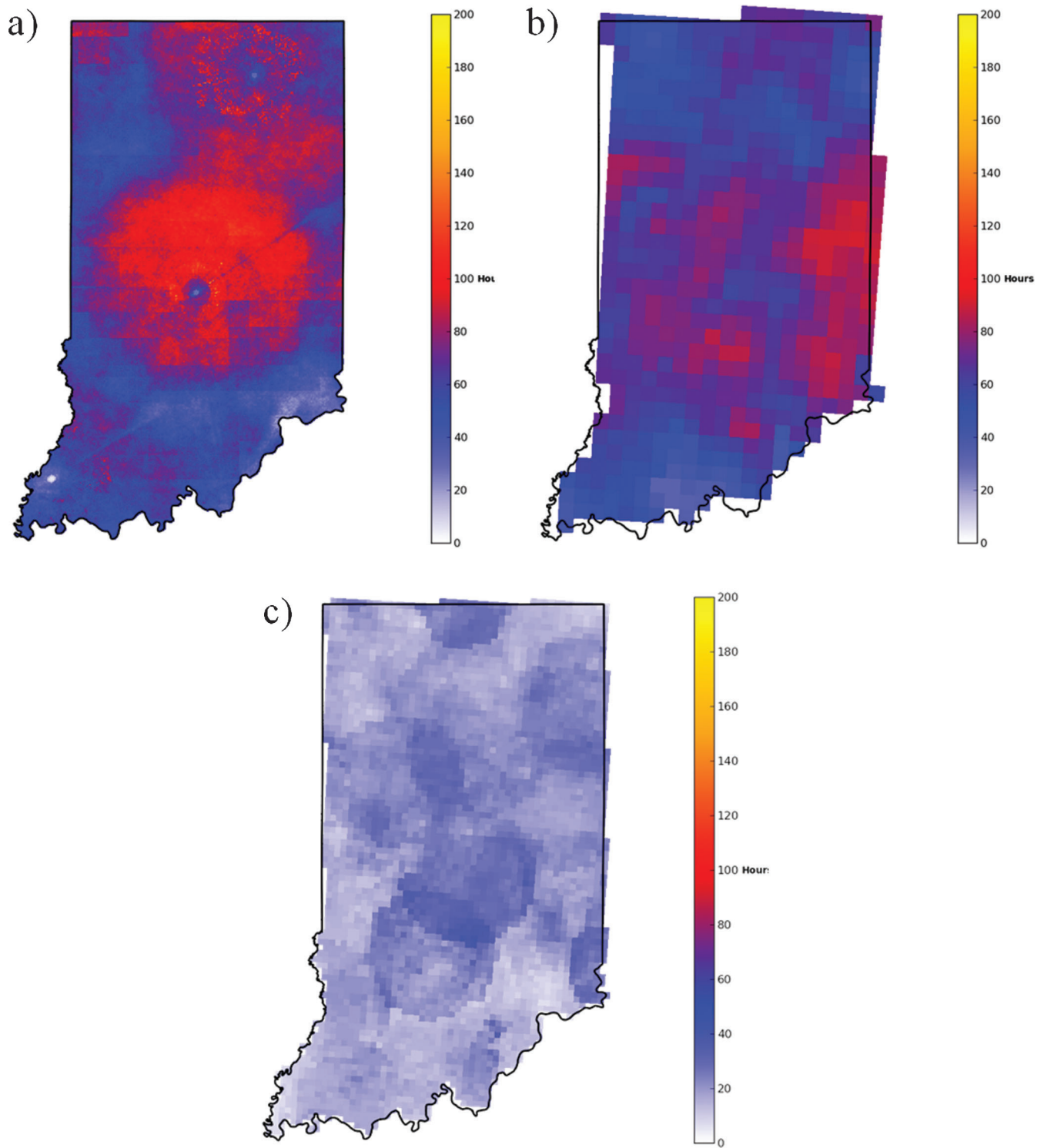
Figure 2.27 March monthly snow hour estimates for 2012–2013 as estimated by (a) NMQ (b) RAP (c) RTMA.

3. ANALYSIS OF DATA: SECTION 2—WINTER WEATHER FORECASTS AND FORECAST EVALUATION

3.1 Experimental Winter Weather Forecasts

Purdue meteorology students (at both the under-graduate and graduate level) helped to design and produce experimental weather forecasts for INDOT during the 2012–2013 winter season. During the Fall 2012 and Spring 2013 semesters, Prof. Baldwin organized his Team Weather Forecasting and Mesoscale Forecasting classes at Purdue to design the forecast products, issue the daily forecasts, and evaluate these experimental forecasts. In the late fall, Prof. Baldwin and his students visited each INDOT district and gave a presentation to INDOT staff regarding winter weather forecasting and the physical processes that produce snow and other types of winter hazards. By communicating directly with INDOT staff through these district-level meetings, the Purdue students were able to design forecast products to benefit their "customers." In addition, the training material was intended to provide information to staff fighting snow and ice to better understand the cloud and precipitation processes. This training should prove most beneficial when the actual observed weather is found to be significantly different than the predicted weather. For example, it is not unusual for a winter storm to contain a wide variety of precipitation types, from rain to sleet to snow, changing over distances as short as the width of a county. The temperatures aloft are a key factor in determining the type of precipitation reaching the ground. Often, a layer of warm air is found above the ground that will melt snow as it falls through the layer. Understanding of how these physical processes of melting and freezing affect the precipitation as it falls from the cloud to the ground will allow staff to react faster and more effectively when an "unexpected" change in the weather occurs at their location.

The daily winter weather forecasts consisted of a state-wide map for the probability of winter weather covering the midnight-midnight period for the next day. Three probability levels were typically used: 30, 60, and 90%. Additional maps were provided for more significant weather events to communicate detailed aspects of the upcoming storm. These included maps of total snowfall, timing of the beginning of the precipitation, locations of freezing rain, etc. In addition to these state-wide probability maps, district-specific forecast "timelines" were provided to indicate the starting and ending times of expected hazards. These hazards included snow, rain, freezing rain, blowing snow, and icing (frost, freezing fog). Different hazards were indicated with different color codes, allowing the forecast to show a change from one hazard to another, or multiple weather types occurring at the same time. A written weather hazard discussion was provided for each district to go along with each timeline. More detailed information was provided in the written discussion, such as specifying which counties were more likely to experience the winter weather, the level of uncertainty in the forecast, and alternate scenarios possible for the upcoming weather event. Finally, an extended forecast was provided to go beyond the next day, discussing the expected weather conditions for the upcoming seven day period. The forecast products were communicated to INDOT via a web page (www.extremeweathermakers.com/indot-forecasts) which was updated daily in the early afternoon, and again in the late evening whenever the situation called for an update to the forecast. Routine weather forecasting began on November 1, 2012 and continued daily throughout the winter, until ending on April 13, 2013.

An example of these forecast products is provided for the case of the winter storm event of March 5–6, 2013. This event was discussed previously in section 1.3 regarding the performance of the HCA algorithm. The state-wide probability of winter weather map (Figure 3.1) was issued one day earlier (March 4). This indicated a strong probability of winter weather across the northern half of the state, with probabilities decreasing further south. The district-level timelines (Figure 3.2) indicate that changing weather conditions were expected throughout the day, with freezing rain conditions possible early across central and northern districts. The central and southern districts showed rain changing to snow with different timings during the course of the day/evening. The written forecast discussion for each district went into more detail regarding the timing of the various types of precipitation, when significant snowfall was expected, and the distribution of snowfall totals across each district. Discussion regarding the possibility for freezing rain during the early morning hours in central Indiana, along with the expected amounts of glaze icing, was also included in the written forecast. Finally, a statewide map of expected snowfall amounts (Figure 3.3) also included some additional text highlighting the changing nature of the expected precipitation during this event.

These forecasts utilized numerical weather predictions that are generated by Prof. Baldwin's research group, using the high-resolution Weather Research and Forecasting (WRF) model which was executed on Purdue's high-performance computing resources twice daily. The Purdue WRF model was run with a grid spacing of 6 km and a domain that covered roughly the eastern 2/3 of the U.S. Forecasts were generated out to 3.5 days into the future, with variables available hourly during the forecast period. Weather-related variables were routinely mapped over the full domain as well as a zoomed view over Indiana. Parameters such as surface temperature, dew point depression, wind, and simulated radar reflectivity were visualized. The numerical forecasts of surface temperature resulted from the WRF model coupling of the NOAH land surface model (15) with the atmospheric components of the WRF. The NOAH land surface model classifies the type of surface at each location within the model domain using a USGS land use database. There are 23 different land surface types available, ranging from
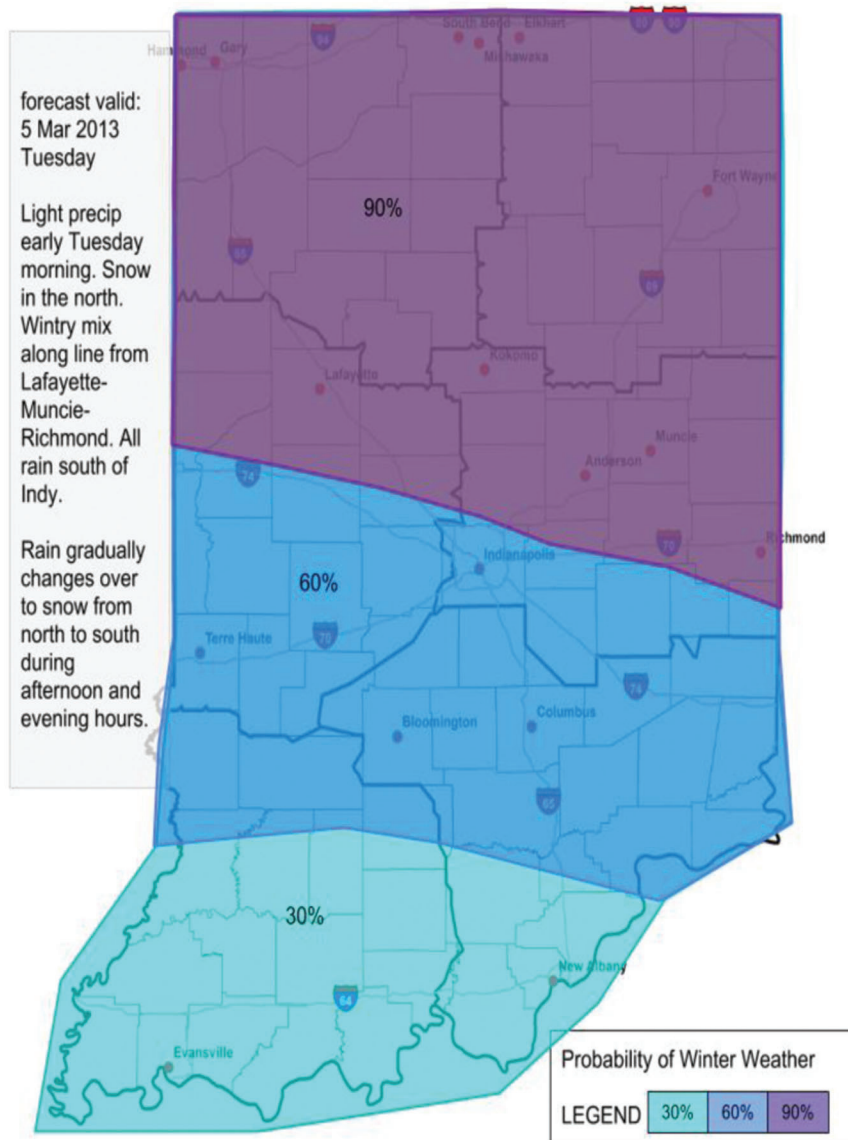
Figure 3.1 Example state-wide winter weather probability map issued 4 Mar 2013, valid for the midnight-midnight period of 5 Mar 2013.

dense forest, agricultural, to urban area. Given the grid spacing of the model that was used during this season (6 km), road surfaces and bridge decks were too small to be resolved; therefore no attempt was made to utilize the characteristics of those types of surfaces in the prediction. Instead, the characteristics of the general land use in each grid area were used to drive the numerical surface temperature predictions. Informal evaluation of the numerical predictions of surface temperatures from the Purdue WRF (compared with RWIS observations) were favorable, providing Purdue forecasters with enough confidence to use those values when creating their forecasts, particular when considering events such as bridge deck frost and freezing fog conditions. Formal statistical evaluation of the WRF surface temperature forecasts is ongoing. The output from this numerical model was routinely available to

INDOT staff via web access (currently found at http://weather.eaps.purdue.edu/wrfdata/).

3.2 Performance Measures for Winter Weather Forecasts

Performance measures for winter weather forecasts were developed using Stage I winter weather analyses (section 1) and the experimental winter weather forecast products described in section 2. Evaluations were performed on two sets of experimental winter weather forecasts, statewide probabilistic winter weather forecasts and hourly timelines of winter weather hazards (rain, snow, freezing rain, and icing/freezing fog) for each INDOT district. More information about these experimental forecast products can be found in the previous section. Evaluation of the probabilistic winter
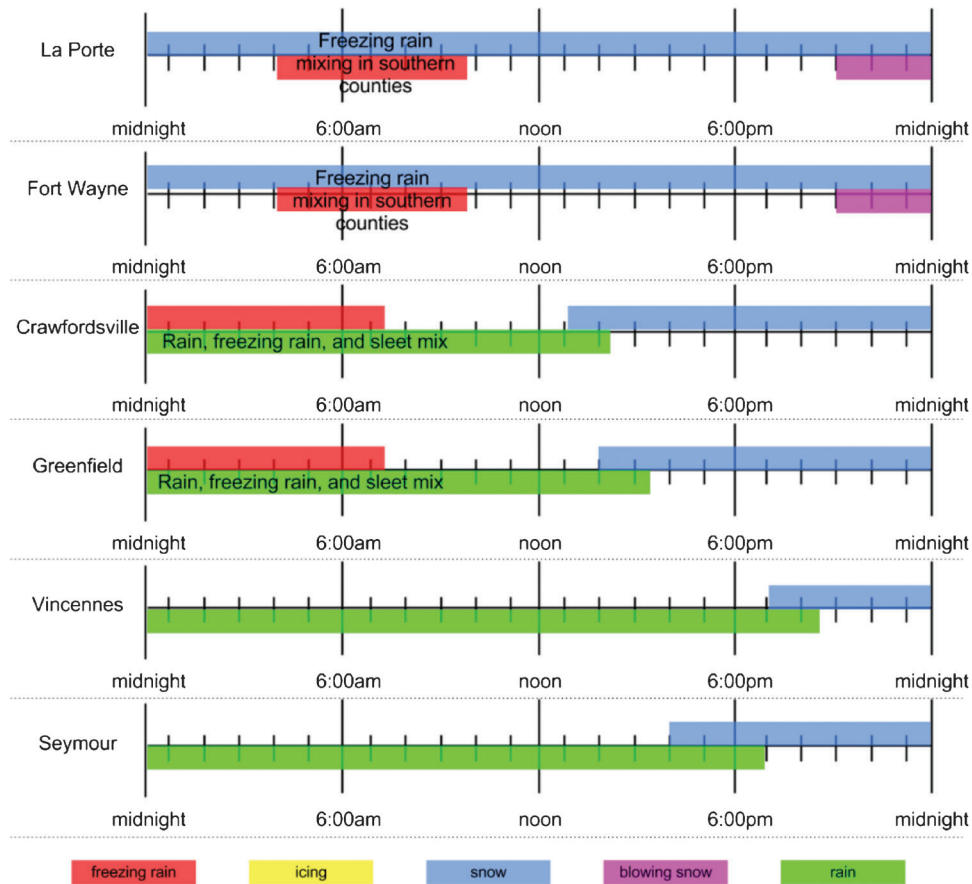
Figure 3.2 Example timeline forecast issued 4 Mar 2013, valid midnight-midnight 5 Mar 2013.

weather forecasts was done using a distributions-based approach and using performance measures developed using a contingency table. Evaluation of timeline forecasts was done using only performance measures developed using a contingency table.

3.2.1 Distributions-Based Forecast Evaluation

Distributions-based forecast evaluation is based upon analysis of the distributions of forecasts and observations (*16*) in terms of joint and conditional probabilities. Distributions-based forecast evaluation provides valuable insight into the performance of forecast systems, especially when examining forecasts that include probabilities. By denoting the set of forecasts as *f* and the corresponding observations as *o*, the joint probability distribution of the forecasts and observations can be denoted as *p(f,o)*. As shown in (*16*), the joint distribution can be factorized to determine the frequency of occurrence of an observed event given the forecasts, or the frequency of forecasts given a set of observations. These are called calibration-refinement factorization and likelihood-base rate factorization, respectively. Calibration-refinement factorization can be expressed mathematically by

$$p(f,o) = p(o|f)p(f) \qquad (1)$$

where $p(o|f)$ is the conditional probability of the observations given each forecast value and $p(f)$ is the marginal distribution of the forecasts. Similarly, likelihood-base rate factorization can be expressed by

$$p(f,o) = p(f|o)p(o) \qquad (2)$$

where $p(f,o)$ is the conditional probability of the forecasts given each observed value and $p(o)$ is the marginal distribution of the observations.

As previously stated, distributions-based forecast evaluation was performed only on the experimental daily probabilistic winter weather forecasts that were provided daily to INDOT by students at Purdue University. Hourly ASOS observations were used to evaluate the daily probabilistic forecasts. Observations from ASOS were overlaid with each day's probabilistic forecast using ArcGIS. Probabilistic forecasts consisted of four forecast probabilities: 0, 30, 60, and 90%. These forecast percentages were used for distributions-based evaluation. Any observation of winter weather (snow, freezing rain, sleet, or freezing fog) was treated as a "yes" observation. Distributions-based forecast
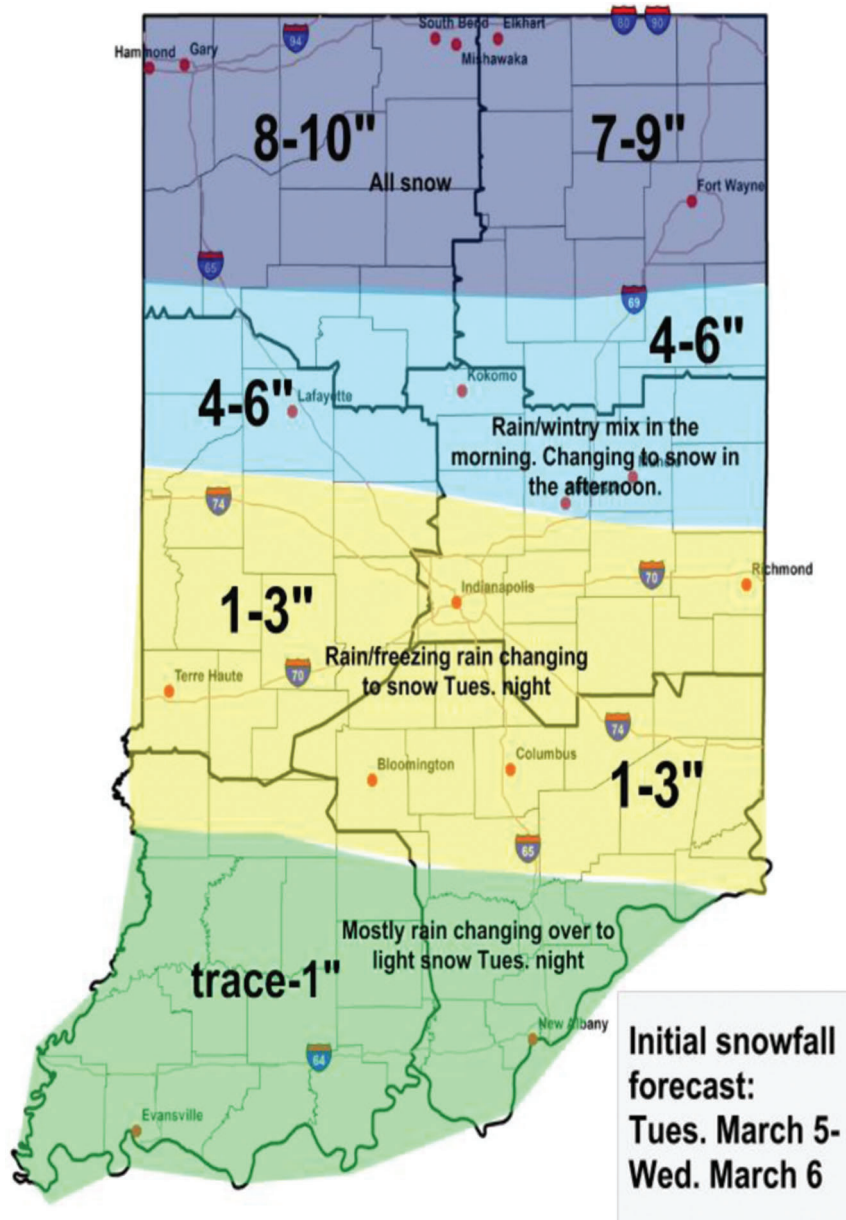
Figure 3.3 Example supplemental forecast map for the Mar 5–6 winter storm.

evaluation was performed by comparing the frequency of different probabilistic forecasts with corresponding observations.

TABLE 3.1
Sample contingency table for verifying a dichotomous forecast

		Observed		
		Yes	No	Total
Forecast	Yes	a	b	$a + b$
	No	c	d	$c + d$
	Total	$a + c$	$b + d$	1

3.2.2 Performance Measures Developed Using Contingency Tables

Typically, "yes" or "no" (dichotomous) forecasts can be evaluated by using contingency tables. An example of a contingency table is shown in Table 3.1. From Table 3.1, a correct "yes" forecast of an observed event (a) is known as a "hit"; a "yes" forecast for an event that did not occur in the observations (b) is a "false alarm"; when an event is observed but "no" was forecast (c) it is a "missed event"; a correct forecast of "no" (d) is called a "correct null." Using the variables (a, b, c, d) from the contingency table, performance measures can be developed (mathematically defined in Table 3.2). Bias is the overall correspondence between the average forecast

TABLE 3.2
Performance measures derived from contingency tables. From (18)

Score	Definition	Range
Bias	$B = \dfrac{a+b}{a+c}$	$0 \le B \le \infty$
Probability of detection	$POD = \dfrac{a}{a+c}$	$0 \le POD \le 1$
Threat score	$TS = \dfrac{a}{a+b+c}$	$0 \le TS \le 1$
Equitable threat score	$ETS = \dfrac{a - a_{rand}}{a+b+c-a_{rand}}$ $rand = \dfrac{(a+b)(a+c)}{a}$	$\dfrac{-1}{3} \le ETS \le 1$
True skill statistic	$TSS = \dfrac{a}{a+c} - \dfrac{b}{b+d}$	$-1 \le TSS \le 1$
Bias-adjusted threat score	$TSA = \dfrac{(a+c)^{1/B} - c^{1/B}}{(a+c)^{1/B} + c^{1/B}}$ $B = \dfrac{a+b}{a+c}$	$0 \le TSA \le 1$
Odds ratio skill score	$ODDS = \dfrac{ad - bc}{ad + bc}$	$-1 \le ODDS \le 1$

and the average observation (17). From (18) the rest of the performance measures are defined. Probability of detection (POD) is the fraction of correct forecasts divided by the total number of "yes" observations. Threat score (TS) is fraction of the union of observed and forecast areas that were corrected forecast. The equitable threat score (ETS) is an adjustment to the threat score that removes correct forecasts that one would expect due to random chance. The true skill statistic (TSS) is equal to the probability of detection minus the probability of false detection (the ratio of false alarms to the number of times no event was observed). The bias-adjusted threat score (TSA) adjusts the threat score to account for bias and is equal to the threat score when bias is 1. The odds ratio skill score (ODDS) is derived from the odds ratio ($=ad/bc$).

Dichotomous forecast verification was also performed on the experimental daily probabilistic forecasts. Any non-zero winter weather forecast was treated as a "yes" forecast of winter weather. Point ASOS observations were used to verify forecasts. If any "yes" observation fell within a non-zero forecast area, it was treated as a correct hit; a correct forecast of no winter weather within an area with no winter weather observations was called a correct null, and so forth until all contingency table values were populated from all sets of forecasts and observations. A similar verification process was performed on the hourly timeline forecasts (24 hour forecasts from 12 a.m. to

12 a.m. local time) made for each INDOT maintenance district. Verification was performed for four forecast variables, snow, freezing rain, icing/freezing fog, and rain. Blowing snow forecasts could not be verified due to a lack of observations. Due to sporadic ASOS observations, verification of the timelines was done on a daily basis instead of an hourly one. If an hourly timeline forecast for a district included a hazard for any part of a day and an observation of that hazard was observed within that district for that same day, regardless of what hour the hazard was forecast, then the forecast was treated as a correct hit, and similarly for each variable of the contingency table.

3.2.3 Results and Discussion

Evaluation of the experimental probabilistic winter weather forecasts is shown in Table 3.3. The calibration-refinement factorization showed that winter weather was observed 26.5% of the time when no winter weather was forecast. The 30% forecast results are even more skewed, with winter weather occurring on 63% of the occasions when a 30% chance of winter weather was forecast. The 60% and 90% forecast factorizations show upward skewing as well with winter weather observed on 81% and 95% of the times, respectively, when forecast. Many forecasters appear to have equated a low probability event with a "low impact" event. For example, a forecaster may have been

TABLE 3.3
Calibration-refinement factorization (left) and likelihood-base rate factorization (right) of daily probabilistic forecasts

		Forecasts							
		0%	30%	60%	90%	0%	30%	60%	90%
Observations	Yes (o = 1)	0.266	0.631	0.811	0.955	0.209	0.399	0.264	0.129
N = 306	No (o = 0)	0.734	0.369	0.189	0.045	0.657	0.266	0.070	0.007

TABLE 3.4
Performance measures for statewide daily probabilistic forecasts

	Bias	POD	TS	ETS	TSS	TSA	ODDS
Score	1.079	0.787	0.608	0.291	0.449	0.614	0.757

confident that a low impact winter weather event would occur, but he or she predicted a 30% of occurrence since the event was expected to cause only minor inconveniences to motorists. These issues will have to be addressed in upcoming winter weather forecasts.

Table 3.4 shows several performance measures computed by contingency table value for the statewide probability forecasts. Overall, the probabilistic forecasts

TABLE 3.5
Performance measures for daily timeline forecasts for the Fort Wayne district

District: Fort Wayne; Hazard: Rain

	Bias	POD	TS	TSS	TSA	ODDS
Score	0.833	0.733	0.667	0.669	0.660	0.951

District: Fort Wayne; Hazard: Freezing Rain

	Bias	POD	TS	TSS	TSA	ODDS
Score	0.833	0.470	0.348	0.423	0.368	0.901

District: Fort Wayne; Hazard: Snow

	Bias	POD	TS	TSS	TSA	ODDS
Score	0.772	0.700	0.650	0.582	0.65	0.892

District: Fort Wayne; Hazard: Freezing Fog

	Bias	POD	TS	TSS	TSA	ODDS
Score	0.813	0.125	0.080	0.040	0.080	0.241

TABLE 3.6
Performance measures for daily timeline forecasts for the La Porte district

District: La Porte; Hazard: Rain

	Bias	POD	TS	TSS	TSA	ODDS
Score	0.860	0.845	0.656	0.654	0.651	0.938

District: La Porte; Hazard: Freezing Rain

	Bias	POD	TS	TSS	TSA	ODDS
Score	0.824	0.958	0.538	0.956	1.000	1.000

District: La Porte; Hazard: Snow

	Bias	POD	TS	TSS	TSA	ODDS
Score	0.774	0.847	0.720	0.720	0.723	0.921

District: La Porte; Hazard: Freezing Fog

	Bias	POD	TS	TSS	TSA	ODDS
Score	0.8125	0.125	0.080	0.053	0.097	0.300

TABLE 3.7
Performance measures for daily timeline forecasts for the Crawfordsville district

District: Crawfordsville; Hazard: Rain

	Bias	POD	TS	TSS	TSA	ODDS
Score	0.943	0.808	0.712	0.735	0.704	0.963

District: Crawfordsville; Hazard: Freezing Rain

	Bias	POD	TS	TSS	TSA	ODDS
Score	4.000	1.000	0.250	0.938	1.000	1.000

District: Crawfordsville; Hazard: Snow

	Bias	POD	TS	TSS	TSA	ODDS
Score	0.977	0.735	0.590	0.614	0.590	0.905

District: Crawfordsville; Hazard: Freezing Fog

	Bias	POD	TS	TSS	TSA	ODDS
Score	1.429	0.286	0.592	0.229	0.117	0.737

were unbiased (near 1), implying that forecasters did not over-forecast winter weather. However, as the previous results showed, forecasters did struggle in assigning reliable probabilistic forecast values, with reliable probabilities showing observed frequencies near the forecast probabilities.

Verification results for each district's daily timeline forecasts are shown in Tables 3.5 through 3.10. Rain and snow forecast forecasts for districts in central and northern Indiana showed a slight low bias in rain and snow forecasts, while snow and rain forecasts for districts in southern Indiana were near 1. Freezing rain forecasts in all districts outside of Seymour and Vincennes showed a severe high bias, to the point where POD was 1 for the Crawfordsville and Vincennes districts.

TABLE 3.8
Performance measures for daily timeline forecasts for the Greenfield district

District: Greenfield; Hazard: Rain

	Bias	POD	TS	TSS	TSA	ODDS
Score	0.780	0.723	0.694	0.690	0.684	0.970

District: Greenfield; Hazard: Freezing Rain

	Bias	POD	TS	TSS	TSA	ODDS
Score	2.200	0.800	0.333	0.747	0.350	0.972

District: Greenfield; Hazard: Snow

	Bias	POD	TS	TSS	TSA	ODDS
Score	0.790	0.667	0.594	0.578	0.602	0.908

District: Greenfield; Hazard: Freezing Fog

	Bias	POD	TS	TSS	TSA	ODDS
Score	0.785	0.143	0.087	0.069	0.098	0.353

TABLE 3.9
Performance measures for daily timeline forecasts for the Vincennes district

District: Vincennes; Hazard: Rain

	Bias	POD	TS	TSS	TSA	ODDS
Score	1.102	0.898	0.746	0.663	0.777	0.933

District: Vincennes; Hazard: Freezing Rain

	Bias	POD	TS	TSS	TSA	ODDS
Score	5.500	1.000	0.182	0.917	1.000	1.000

District: Vincennes; Hazard: Snow

	Bias	POD	TS	TSS	TSA	ODDS
Score	1.069	0.655	0.463	0.507	0.461	0.832

District: Vincennes; Hazard: Freezing Fog

	Bias	POD	TS	TSS	TSA	ODDS
Score	1.289	0.574	0.333	0.523	0.318	0.926

TABLE 3.10
Performance measures for daily timeline forecasts for the Seymour district

District: Seymour; Hazard: Rain

	Bias	POD	TS	TSS	TSA	ODDS
Score	1.086	0.897	0.754	0.697	0.780	0.944

District: Seymour; Hazard: Freezing Rain

	Bias	POD	TS	TSS	TSA	ODDS
Score	3.667	0.333	0.077	0.242	0.055	0.667

District: Seymour; Hazard: Snow

	Bias	POD	TS	TSS	TSA	ODDS
Score	1.059	0.794	0.628	0.680	0.633	0.936

District: Seymour; Hazard: Freezing Fog

	Bias	POD	TS	TSS	TSA	ODDS

However, in the Seymour district false alarms were numerous, lowering all skill scores. Freezing fog forecasts clearly performed the worst, with several skill scores near zero for multiple districts. Some of the low scores could be due to a paucity of ASOS observations; forecasts for freezing fog and icing were often issued when bridge deck frost formation was expected, the airport observations will not provide information to indicate if road surface frost actually occurred. Output from Purdue's Weather Research and Forecasting (WRF) model were used in forecasting icing and freezing fog, and more information about the numerical surface temperature forecasts can be found in section 2.1.

Overall, rain and snow forecasts were shown to be the most skillful forecast produced for INDOT, with freezing rain forecasts marginally. Some caution should be taken into making inferences on forecasts based on one skill score alone. Most skill scores are sensitive to event frequency and bias. Scores are likely skewed for highly biased forecasts (e.g. freezing rain). Additionally, rain and snow were far more common than freezing rain and freezing fog/icing observations. This skews most skill scores lower for freezing rain and icing because they were the rarer of the four forecast hazards.

4. CONCLUSIONS

The objectives for this project were to provide INDOT with more detailed forms of weather information, for both monitoring and forecasting purposes. Several "state-of-the-art" weather analyses were evaluated and compared against surface station observations to determine which system would generate weather hour estimates that were both accurate and spatially detailed. The RTMA-based analyses underestimated weather hours and also contained analysis artifacts (circular patterns) that were unrealistic. The NMQ-based analyses over-estimated weather hours, especially within ~75 miles of a radar site, except for a narrow circle centered at each NWS radar location. The NWS dual-pol radar products were found to be immature with the precipitation type classification algorithm containing several major errors. The RAP-based weather hour analyses matched up well against the surface station data and also provided more realistic spatial detail. These analyses are recommended for use for after-action review both for previous and upcoming winter seasons.

Experimental winter weather forecasts were provided to INDOT by Purdue students (under the supervision of Prof. Baldwin). These forecast products were evaluated and were found to be skillful and unbiased in predicting the occurrence of snow in particular. Purdue students (and professors) gained a rich learning experience as a result of their interaction with their INDOT "customers," it is recommended that Purdue continues to communicate this kind of weather forecast information to INDOT for upcoming winter seasons. High-resolution numerical weather prediction model output was also incorporated into these experimental forecast products. These numerical forecasts were found to be very useful by the Purdue student forecasters. It is recommended that Purdue continue to evaluate and develop numerical weather forecasts for road weather purposes, working with INDOT's weather vendor to provide direct access to this alternate source of forecast information, resulting in increased confidence and improved decision-making for winter maintenance.

5. RECOMMENDATIONS

In order to take advantage of the detailed spatial information contained in the radar-based estimates of precipitation, it is recommended that INDOT begin to use the RAP-based analysis variables in their winter

weather hour calculations. Purdue researchers will provide these data in a form that can easily be utilized in INDOT's GIS system, which will allow INDOT staff to use the more detailed information in their analysis of costs of winter maintenance operations. This detailed information will provide a more precise representation of the actual weather conditions as they varied within each district, from unit to unit. By providing this information for the past several years, INDOT will be able to go back and analyze previous winter seasons, increasing the opportunities for determining which areas of the state are providing the most cost-effective service.

It is recommended that INDOT continue to utilize the winter weather forecasting information provided by Purdue students, while also incorporating the numerical forecast information from the Purdue WRF model. This additional forecast information should be used in addition to the various weather forecasting sources that are currently utilized by INDOT staff, including weather vendors, local media, web sites, and National Weather Service products. In the field of weather prediction, we find that a consensus-based forecast from multiple sources outperforms those from any single individual source. The student-generated forecasts are designed for direct use in INDOT winter maintenance decision-making, taking into account the forecast information available from multiple sources. In order to improve the access and ease-of-use of the numerical forecast information from the Purdue WRF model, it is recommended that INDOT encourage their weather vendor to collaborate with Purdue researchers to bring the numerical information directly into their systems, allowing INDOT direct access to that information via their MDSS.

6. EXPECTED BENEFITS, DELIVERABLES, IMPLEMENTATION, AND COST SAVINGS

The main deliverables from this project are new, more detailed datasets for analyzing winter weather hours across the state. These data will be provided to INDOT in a form that will allow easy implementation into INDOT GIS analysis systems. We recommend that INDOT begin using the more detailed analysis datasets to analyze the performance of maintenance operations for upcoming and previous winter seasons. Results from evaluation of the new dual-pol radar products have shown that the algorithmic classifications of precipitation types are often erroneous. These products are immature in their development; we recommend that INDOT delay implementation of the dual-pol radar products until further improvements can be implemented by the National Weather Service. Another main deliverable from this project is numerical forecast information from the Purdue WRF model; we recommended that INDOT encourage their weather vendor to collaborate with Purdue researchers to bring the numerical information directly into their systems, allowing INDOT direct access to that information via

their MDSS. A third deliverable was student-generated weather forecasts that were designed for direct use in INDOT winter maintenance decision-making, taking into account the forecast information available from multiple sources. One of the main results from the evaluation of Purdue's experimental weather forecasts was that these forecasts were, on average, unbiased in terms of the frequency of occurrence of snow at the district level. Unbiased forecasts, or forecasts that do not either over-forecast or under-forecast the frequency of winter weather conditions, should help to minimize unnecessary costs due to extra man hours/overtime.

Many costs associated with winter maintenance cannot be avoided, a larger number of weather hours will require and larger number of hours spent fighting snow and ice. However, lessons can be learned and best practices can be implemented from unit-to-unit. With more accurate and precise estimates of winter weather hours, analysis of costs per lane mile per weather hour will improve, allowing the potential more uniform (and cost-effective) operations state-wide. While it is unreasonable to expect that every sub-district could reach a goal of uniform costs per lane mile per weather hour, one can assume that the sub-districts currently showing costs per lane mile per weather hour above the state average could reduce their costs as a result of applying those best practices learned from more cost-effective sub-districts. Using the current INDOT weather hour estimate, if those above average sub-districts were to reduce their costs a point halfway in between their current (2012–2013) expenses and the overall state average cost per lane mile per weather hour, the overall savings would be in the 3–4% range over the course of an entire winter season. These estimates will change if more detailed weather hour estimates are used, since these will provide a more accurate local estimation of the weather conditions at the sub-district and unit level.

REFERENCES

1. Kwon, T. J., L. Fu, and C. Jiang. Effect of Winter Weather and Road Surface Conditions on Macroscopic Traffic Parameters. In *Transportation Research Record: Journal of the Transportation Research Board*, No. 2329, Transportation Research Board of the National Academies, Washington, D.C., 2013, pp. 54–62. doi: 10.3141/2329-07.

2. ESRI. *IDW (Geostatistical Analyst)*, 2011. http://help.arcgis.com/en/arcgisdesktop/10.0/help/index.html#//003000000007000000.htm. Accessed April 22, 2013.

3. ESRI. *How inverse distance weighted interpolation works*. 2011. http://help.arcgis.com/en/arcgisdesktop/10.0/help/index.html#//00310000002m000000.htm. Accessed April 22, 2013.

4. ESRI. *Performing cross-validation and validation*. http://help.arcgis.com/en/arcgisdesktop/10.0/help/index.html#//003100000059000000.htm. Accessed April 22, 2013.

5. De Pondeca, M. S. F. V., et al. The Real-Time Mesoscale Analysis at NOAA's National Centers for Environmental Prediction: Current Status and Development. *Weather and Forecasting*, Vol. 26, No. 5, 2011, pp. 593–612. doi: 10.1175/WAF-D-10-05037.1.

6. Lin, Y., and K. E. Mitchell. The NCEP Stage II/IV Hourly Precipitation Analyses: Development and Applications. Presented at the 19th Conference on Hydrology San Diego, CA, American Meteorology Society, Jan. 10, 2005. http://ams.confex.com/ams/pdfpapers/83847.pdf.

7. Zhang, J., K. Howard, et al. National Mosaic and Multi-Sensor QPE (NMQ) System: Description, Results, and Future Plans. *Bulletin of the American Meteorological Society*, Vol. 92, No. 10, 2011, pp. 1321–1338. doi: 10.1175/2011BAMS-D-11-00047.1

8. Rinehart, R. E. *Radar for Meteorologists*. 4th ed., Rinehart Publications, 2004.

9. Bringi, V. N., and V. Chandrasekar. *Polarimetric Doppler Weather Radar: Principles and Applications*. 2nd ed. Cambridge University Press, Cambridge, 2001.

10. NOAA. Radar Operations Center, WSR-88D Build 10/Super Resolution Level II FAQs, Oct. 19, 2007. http://www.roc.noaa.gov/wsr88d/BuildInfo/Build10FAQ.aspx.

11. Doviak, R. J., and D. S. Zrnić. *Doppler Radar and Weather Observations*. 2nd ed. Dover Publications, Mineola, 1993.

12. Vincenty, T. Direct and Inverse Solutions of Geodesics on the Ellipsoid with application of nested equations. *Survey Review*, Vol. 23, No. 176, 1975, pp. 88–93. http://www.ngs.noaa.gov/PUBS_LIB/inverse.pdf

13. Park, H. S., A. V. Ryzhkov, D. S. Zrnić, and K.-E. Kim. The Hydrometeor Classification Algorithm for the Polarimetric WSR-88D: Description and Application to an MCS. *Weather and Forecasting*, Vol. 24, No. 3, 2009, pp. 730–748. doi: 10.1175/2008WAF2222205.1

14. Elmore, K. L. The NSSL Hydrometeor Classification Algorithm in Winter Surface Precipitation: Evaluation and Future Development. *Weather and Forecasting*, Vol. 26, No. 5, 2011, pp. 756–765. doi: 10.1175/WAF-D-10-05011.1.

15. Chen, F., Z. Janjić, and K. Mitchell. Impact of Atmospheric Surface-layer Parameterizations in the New Land-surface Scheme of the NCEP Mesoscale Eta Model. *Boundary-Layer Meteorology*, Vol. 85, No. 3, 1997, pp. 391–421. doi: 10.1023/A:1000531001463.

16. Murphy, A. H., and R. L. Winkler. A General Framework for Forecast Verification. *Monthly Weather Review*, Vol. 115, No. 7, 1987, pp. 1330–1338. doi: 10.1175/1520-0493(1987)115<1330%3AAGFFFV>2.0.CO%3B2.

17. Murphy, A. H. What Is a Good Forecast? An Essay on the Nature of Goodness in Weather Forecasting. *Weather and Forecasting*, Vol. 8, No. 2, 1993, pp. 281–293. doi: 10.1175/1520-0434(1993)008%3C0281:WIAGFA%3E2.0.CO;2.

18. Baldwin, M. E., and J. S. Kain. Sensitivity of Several Performance Measures to Displacement Error, Bias, and Event Frequency. *Weather and Forecasting*, Vol. 21, No. 4, 2006, pp. 636–648. doi: 10.1175/WAF933.1.

Tables A.1, A.2, and A.3 list the date and time (YYYYMMDD HHmm) of missing data files from each data source for the past three winter seasons.

TABLE A.1
RAP/RUC

2010–2011			2011–2012	2012–2013
20101110 2000	20101114 0000	20110303 2300	20120105 1800	20121101 2300
20101110 2100	20101114 0100	20110304 0000	20120105 1900	20121123 2300
20101110 2200	20101114 0200	20110304 0100	20120105 2000	20121128 2300
20101110 2300	20101114 0300	20110304 0200	20120105 2100	20121225 2300
20101111 0000	20101114 0400	20110304 0300	20120105 2200	20130120 2300
20101111 0100	20101114 0500	20110304 0400	20120105 2300	20130202 2300
20101111 0200	20101114 0600	20110304 0500	20120107 0000	20130322 2300
20101111 0300	20101114 0700	20110304 0600	20120107 0100	20130327 2300
20101111 0400	20101114 0800	20110304 0700	20120107 0200	
20101111 0500	20101114 0900	20110304 0800	20120107 0300	
20101111 0600	20101114 1000	20110304 0900	20120107 0400	
20101111 0700	20101114 1100	20110304 1000	20120107 0500	
20101111 0800	20101114 1200	20110304 1100	20120107 0600	
20101111 0900	20101114 1300	20110304 1200	20120107 0700	
20101111 1000	20101114 1400	20110304 1300	20120107 0800	
20101111 1100	20101114 1500	20110304 1400	20120107 0900	
20101111 1200	20101114 1600	20110304 1500	20120107 1000	
20101111 1300	20101114 1700	20110304 1600	20120107 1100	
20101111 1400	20101114 1800	20110304 1700	20120107 1200	
20101111 1500	20101114 1900	20110304 1800	20120107 1300	
20101111 1600	20101114 2000	20110304 1900	20120107 1400	
20101111 1700	20101114 2100	20110304 2000	20120107 1500	
20101111 1800	20101114 2200	20110304 2100	20120107 1600	
20101111 1900	20101115 1600	20110304 2200	20120107 1700	
20101111 2000	20110227 0000	20110304 2300	20120107 1800	
20101111 2100	20110227 0100	20110305 0000	20120107 1900	
20101111 2200	20110227 0200	20110305 0100	20120107 2000	
20101111 2300	20110227 0300	20110305 0200	20120107 2100	
20101112 0000	20110227 0400	20110305 0300	20120107 2200	
20101112 0100	20110227 0500	20110305 0400	20120107 2300	
20101112 0200	20110227 0600	20110305 0500	20120109 0000	
20101112 0300	20110227 0700	20110305 0600	20120109 0100	
20101112 0400	20110227 0800	20110305 0700	20120109 0200	
20101112 0500	20110227 0900	20110305 0800	20120109 0300	
20101112 0600	20110227 1000	20110305 0900	20120109 0400	
20101112 0700	20110227 1100	20110305 1000	20120109 0500	
20101112 0800	20110227 1200	20110305 1100	20120109 0600	
20101112 0900	20110227 1300	20110305 1200	20120109 0700	
20101112 1000	20110227 1400	20110305 1300	20120109 0800	
20101112 1100	20110227 1500	20110305 1400	20120109 0900	
20101112 1200	20110227 1600	20110305 1500	20120109 1000	
20101112 1300	20110227 1700	20110305 1600	20120109 1100	
20101112 1400	20110227 1800	20110305 1700	20120109 1200	
20101112 1500	20110227 1900	20110305 1800	20120109 1300	
20101112 1600	20110227 2000	20110305 1900	20120109 1400	
20101112 1700	20110227 2100	20110305 2000	20120109 1500	
20101112 1800	20110227 2200	20110305 2100	20120109 1600	
20101112 1900	20110227 2300	20110305 2200	20120109 1700	
20101112 2000	20110301 2300	20110305 2300	20120109 1800	
20101112 2100	20110302 2000	20110306 0000	20120109 1900	
20101112 2200	20110302 2100	20110306 0100	20120109 2000	
20101112 2300	20110302 2200	20110306 0200	20120109 2100	

2010–2011			2011–2012	2012–2013
20101113 0000	20110302 2300	20110306 0300	20120109 2200	
20101113 0100	20110303 0000	20110306 0400	20120109 2300	
20101113 0200	20110303 0100	20110306 0500	20120306 0900	
20101113 0300	20110303 0200	20110306 0600	20120306 1000	
20101113 0400	20110303 0300	20110306 0700	20120306 1100	
20101113 0500	20110303 0400	20110306 0800	20120306 1200	
20101113 0600	20110303 0500	20110306 0900	20120306 1300	
20101113 0700	20110303 0600	20110306 1000	20120306 1400	
20101113 0800	20110303 0700	20110306 1100	20120306 1500	
20101113 0900	20110303 0800	20110306 1200	20120306 1600	
20101113 1000	20110303 0900	20110306 1300	20120306 1700	
20101113 1100	20110303 1000	20110306 1400	20120322 2200	
20101113 1200	20110303 1100	20110306 1500		
20101113 1300	20110303 1200	20110306 1600		
20101113 1400	20110303 1300	20110306 1700		
20101113 1500	20110303 1400	20110306 1800		
20101113 1600	20110303 1500	20110306 1900		
20101113 1700	20110303 1600	20110306 2000		
20101113 1800	20110303 1700	20110306 2100		
20101113 1900	20110303 1800	20110306 2200		
20101113 2000	20110303 1900	20110306 2300		
20101113 2100	20110303 2000	20110308 0400		
20101113 2200	20110303 2100	20110309 0400		
20101113 2300	20110303 2200	20110313 0400		

TABLE A.2
RTMA

2010–2011			2011–2012	2012–2013
20101220 0500	20110117 0000	20110128 1100	20120130 0000	20121211 1900
20101220 0600	20110117 0100	20110128 1200	20120130 0100	20121211 2000
20101220 0700	20110117 0200	20110128 1300	20120130 0200	20121211 2100
20101220 0800	20110117 0300	20110128 1400	20120130 0300	20121211 2200
20101220 0900	20110117 0400	20110128 1500	20120130 0400	20121211 2300
20101220 1000	20110117 0500	20110128 1600	20120130 0500	
20101220 1100	20110117 0600	20110128 1700	20120130 0600	
20101220 1200	20110117 0700	20110128 1800	20120130 0700	
20101220 1300	20110117 0800	20110128 1900	20120130 0800	
20101220 1400	20110117 0900	20110128 2000	20120130 0900	
20101220 1500	20110117 1000	20110128 2100	20120130 1000	
20101220 1600	20110117 1100	20110128 2200	20120130 1100	
20101220 1700	20110117 1200	20110128 2300	20120130 1200	
20101220 1800	20110117 1300	20110129 0000	20120130 1300	
20101222 1800	20110122 0200	20110129 0100	20120130 1400	
20110114 0500	20110122 0300	20110129 0200	20120130 1500	
20110114 0600	20110122 0400	20110129 0300	20120130 1600	
20110114 0700	20110122 0500	20110129 0400	20120130 1700	
20110114 0800	20110122 0600	20110129 0500	20120130 1800	
20110114 0900	20110122 0700	20110129 0600	20120130 1900	
20110114 1000	20110122 0800	20110129 0700	20120130 2000	
20110114 1100	20110122 0900	20110129 0800	20120130 2100	
20110114 1200	20110122 1000	20110129 0900	20120130 2200	
20110116 1000	20110122 1100	20110129 1000	20120130 2300	
20110116 1100	20110122 1200	20110129 1100	20120131 0000	
20110116 1200	20110122 1300	20110129 1200	20120131 0100	
20110116 1300	20110122 1400	20110129 1300	20120131 0200	
20110116 1400	20110122 1500	20110129 1400	20120131 0300	
20110116 1500	20110122 1600	20110129 1500	20120131 0400	
20110116 1600	20110122 1700	20110129 1600	20120131 0500	
20110116 1700	20110122 1800	20110129 1700	20120131 0600	
20110116 1800	20110122 1900	20110129 1800	20120131 0700	
20110116 1900	20110122 2000	20110129 1900	20120131 0800	
20110116 2000	20110122 2100	20110129 2000	20120131 0900	
20110116 2100	20110122 2200	20110129 2100	20120131 1000	
20110116 2200	20110122 2300	20110129 2200	20120131 1100	
20110116 2300	20110128 1000		20120131 1200	
			20120131 1300	
			20120131 1400	
			20120131 1500	
			20120131 1600	
			20120131 1700	
			20120131 1800	
			20120131 1900	
			20120131 2000	
			20120131 2100	
			20120131 2200	
			20120131 2300	

Joint Transportation Research Program Technical Report FHWA/IN/JTRP-2013/22

TABLE A.3
NMQ

2012–2013
20121214 0800
20121214 0900
20121214 1000
20121214 1100
20121214 1200
20121214 1300
20121214 1400
20121214 1500
20121214 1600
20121214 1700
20121214 1800
20121214 1900
20121214 2000
20121214 2100
20121217 2200

APPENDIX B. VINCENTY DIRECT FORMULA

DESCRIPTION

Vincenty (*12*) demonstrates the two iterative formulae for both the direct and inverse geodetic solutions. Both equations assume the Earth is an oblate spheroid. The method presented in Table B.1 is the direct method; this formula computes the latitude and longitude of a point given the location of a starting point, the distance from the starting point, and the azimuth between the two points.

FORMULATION (FOLLOWING VINCENTY (*12*))

$$tan\, U_1 = (1-f)\, tan\varphi_1$$

$$\sigma_1 = tan^{-1}\left(\frac{tan\, U_1}{cos\alpha_1}\right)$$

$$sina = cos\, U_1 sin\alpha_1$$

$$cos^2\alpha = (1-sin\alpha)(1+sin\alpha)$$

$$u^2 = cos^2\alpha\left(\frac{a^2-b^2}{a^2}\right)$$

$$A = 1 + \frac{u^2}{16384}\left\{4096 + u^2\left[-768 + u^2\left(320 - 175u^2\right)\right]\right\}$$

$$B = \frac{u^2}{1024}\left\{256 + u^2\left[-128 + u^2\left(74 - 47u^2\right)\right]\right\}$$

Using an initial value of $\sigma = \frac{s}{bA}$, the following equations are iterated until no significant change in σ occurs. In this case,

however, the equations are iterated a fixed number of times (here, twenty).

$$2\sigma_m = 2\sigma_1 + \sigma$$

$$\Delta\sigma = Bsin\sigma\{cos(2\sigma_m)$$
$$+ \frac{1}{4}B[cos\sigma\left(-1+2cos^2(2\sigma_m)\right)$$
$$- \frac{1}{6}Bcos(2\sigma_m)\left(-3+4sin^2\sigma\right)\left(-3+4cos^2(2\sigma_m)\right))]\}$$

$$\sigma = \frac{s}{bA} + \Delta\sigma$$

After iteration is completed,

$$\varphi_2 = tan^{-1}\left(\frac{sin\, U_1 cos\sigma + cos\, U_1 sin\sigma cos\alpha_1}{(1-f)\sqrt{sin^2\alpha + (sin\, U_1 sin\sigma - cos\, U_1 cos\sigma cos\alpha_1)^2}}\right)$$

$$\lambda = tan^{-1}\left(\frac{sin\sigma sin\alpha_1}{cos\, U_1 cos\sigma - sin\, U_1 sin\,\sigma cos\alpha_1}\right)$$

$$C = \frac{f}{16}cos^2\alpha\left[4 + f\left(4 - 3cos^2\alpha\right)\right]$$

$$L = \lambda - (1-C)$$
$$f sin\alpha\{\sigma + Csin\sigma\left[cos(2\sigma_m) + Ccos\sigma\left(-1+2cos^2(2\sigma_m)\right)\right]\}$$

$$\alpha_2 = tan^{-1}\left(\frac{sin\alpha}{-sin\, U_1 sin\,\sigma + cos\, U_1 cos\sigma cos\alpha_1}\right)$$

TABLE B.1
Variable Notation

Symbol	Description
a, b	Major length of ellipsoidal Earth (radius at equator) A= 6378137.0 m in WGS-84
f	Flattening of ellipsoid $f = (a-b)/a$
b	Length of minor axis of ellipsoid (radius at Earth's poles)
φ_1, φ_2	Geodetic latitude, north of the equator
L	Difference in longitude between the two points
s	Length of the geodesic (i.e., ellipsoidal distance between the two points)
α_1, α_2	Forward azimuths at each point (clockwise from north)
α	Azimuth at the equator
u^2	$cos^2\alpha\left(\frac{a^2-b^2}{b^2}\right)$
U	Reduced latitude $tan\, U = (1-f)\, tan\,\varphi$
λ	Difference in longitude on the auxiliary sphere
σ	Angular distance on the sphere between two points (arc length)
σ_1	Angular distance on the sphere between the equator and point 1
σ_m	Angular distance on the sphere from the equator to the midpoint of the line between the two points

About the Joint Transportation Research Program (JTRP)

On March 11, 1937, the Indiana Legislature passed an act which authorized the Indiana State Highway Commission to cooperate with and assist Purdue University in developing the best methods of improving and maintaining the highways of the state and the respective counties thereof. That collaborative effort was called the Joint Highway Research Project (JHRP). In 1997 the collaborative venture was renamed as the Joint Transportation Research Program (JTRP) to reflect the state and national efforts to integrate the management and operation of various transportation modes.

The first studies of JHRP were concerned with Test Road No. 1—evaluation of the weathering characteristics of stabilized materials. After World War II, the JHRP program grew substantially and was regularly producing technical reports. Over 1,500 technical reports are now available, published as part of the JHRP and subsequently JTRP collaborative venture between Purdue University and what is now the Indiana Department of Transportation.

Free online access to all reports is provided through a unique collaboration between JTRP and Purdue Libraries. These are available at: http://docs.lib.purdue.edu/jtrp

Further information about JTRP and its current research program is available at: http://www.purdue.edu/jtrp

About This Report

An open access version of this publication is available online. This can be most easily located using the Digital Object Identifier (doi) listed below. Pre-2011 publications that include color illustrations are available online in color but are printed only in grayscale.

The recommended citation for this publication is:

Baldwin, M., K. Hoogewind, D. Snyder, M. Price, and R. J. Trapp. *Assessment and Recommendations for Using High-Resolution Weather Information to Improve Winter Maintenance Operations*. Publication FHWA/IN/JTRP-2013/22. Joint Transportation Research Program, Indiana Department of Transportation and Purdue University, West Lafayette, Indiana, 2013. doi: 10.5703/1288284315224.